

A photograph of a blazar jet, showing a bright, multi-colored (yellow, orange, red, and blue) jet of plasma extending from a central point into a dark, starry space. The jet is oriented diagonally from the bottom left towards the top right.

Physical Properties of Blazar Jets from VLBI Observations

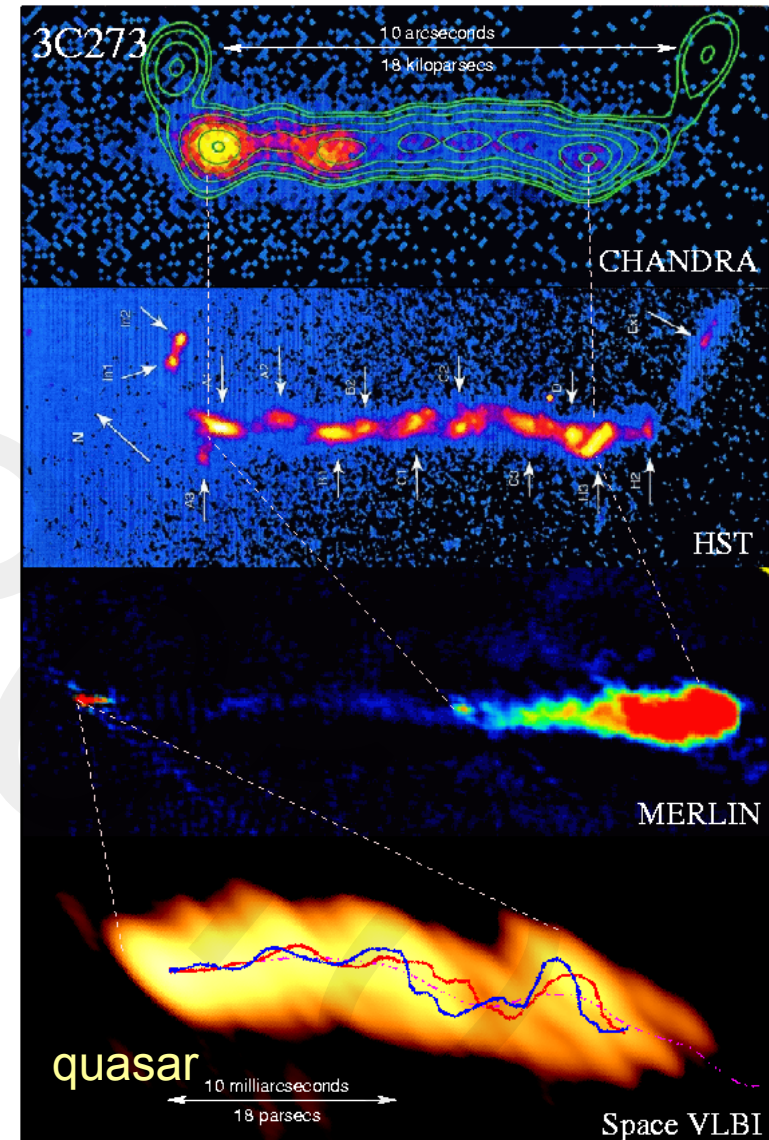
Andrei Lobanov

MPIfR Bonn



Bipolar Outflows

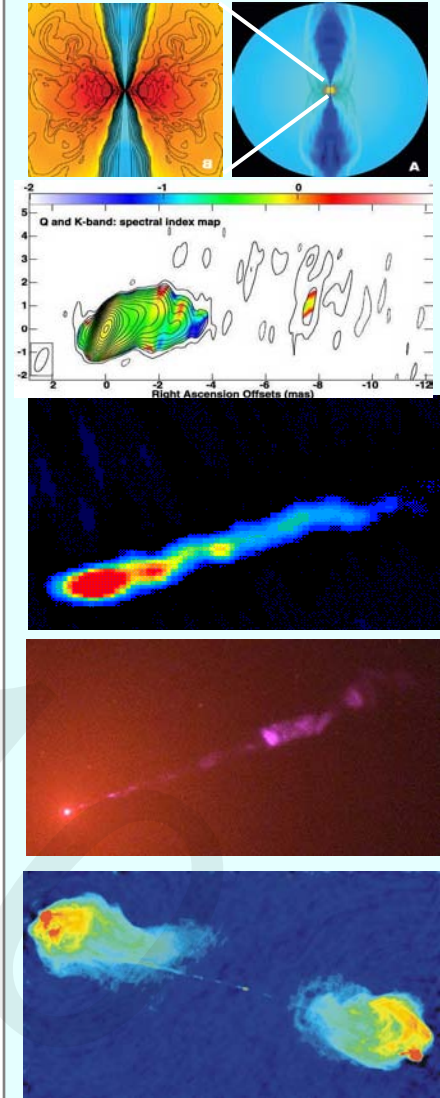
- ❑ Bipolar outflows (jets) are common. They have been found in galactic nuclei, pulsars, and stars (including the Sun).
- ❑ Generally: bipolar outflows solve the problem of transporting excess energy and angular momentum from compact, rotating, magnetized objects which accrete external matter





Basics of AGN Jets

- Launching Region: The Accretion Flow;**
 $\sim 10 - 100 R_g$: $0.05 - 0.5 \text{ mpc}^*$, $0.01 - 0.1 \mu\text{as}^*$
 - Probably unresolved or slightly resolved
- MHD Acceleration/Collimation Region:**
 $\sim 10 - 10^3 R_g$: $0.05 - 5 \text{ mpc}$, $0.01 - 1 \mu\text{as}$
 - The Jet “Nozzle”
- Transition Region:**
 $\sim 10^3 R_g$: $\sim 5 \text{ mpc}$, $\sim 1 \mu\text{as}$
 - Poynting-Flux-Dominated (PFD) \rightarrow KFD
- Kinetic-Flux-Dominated (KFD) Jet:**
 $\sim 10^3 - 10^9 R_g$: $5 \text{ mpc} - 5 \text{ kpc}$, $1 \mu\text{as} - 1''$
- Hot Spot/Lobe:**
 $> 10^9 - 10^{10} R_g$: $5 - 50 \text{ kpc}$, $1 - 10''$
 - Outer jet is Kinetic-Flux-Dominated

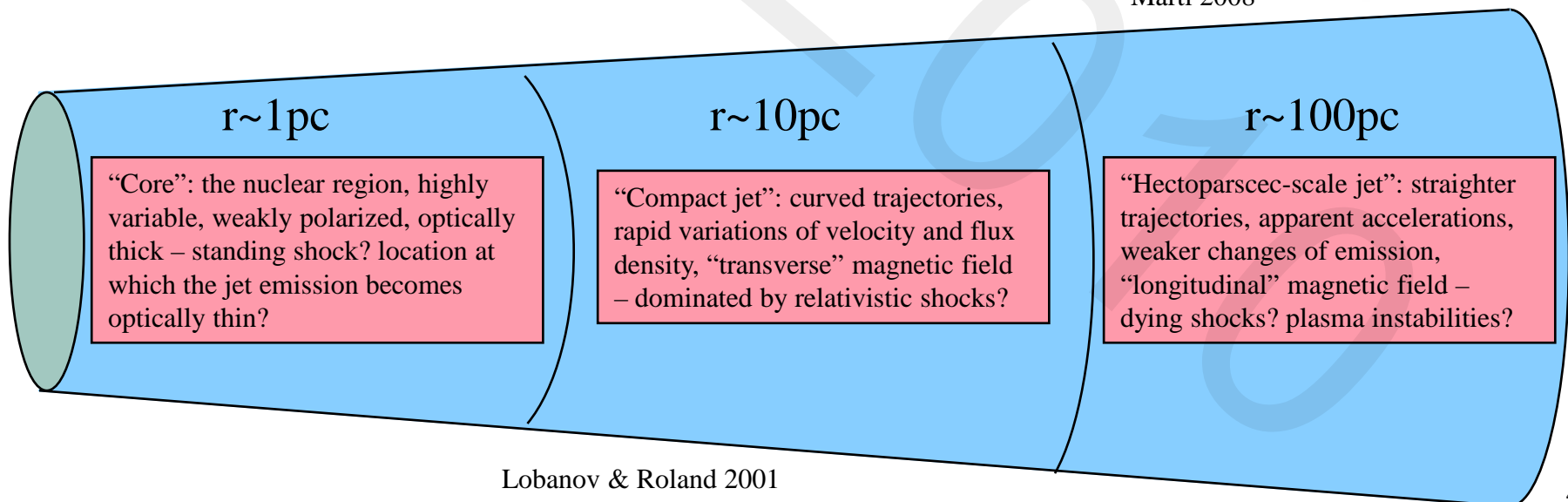
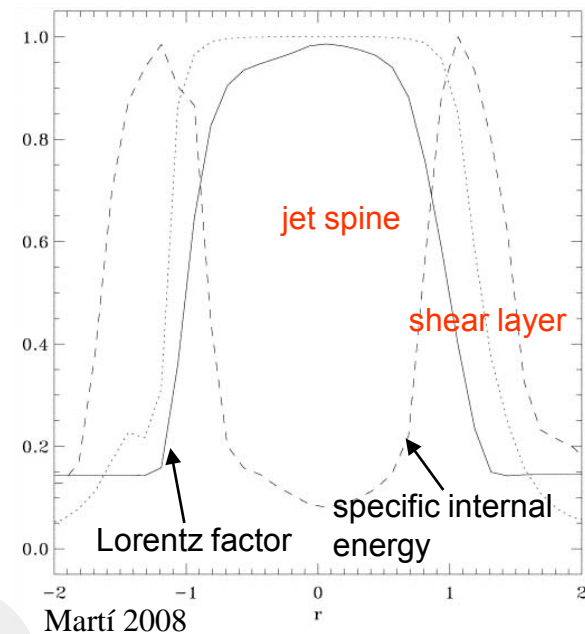


For a black hole of $10^8 M_{\text{sun}}$ at 1 Gpc (in M87: $10 R_g \sim 0.02 \text{ mas}$)



"Flowing" Paradigm

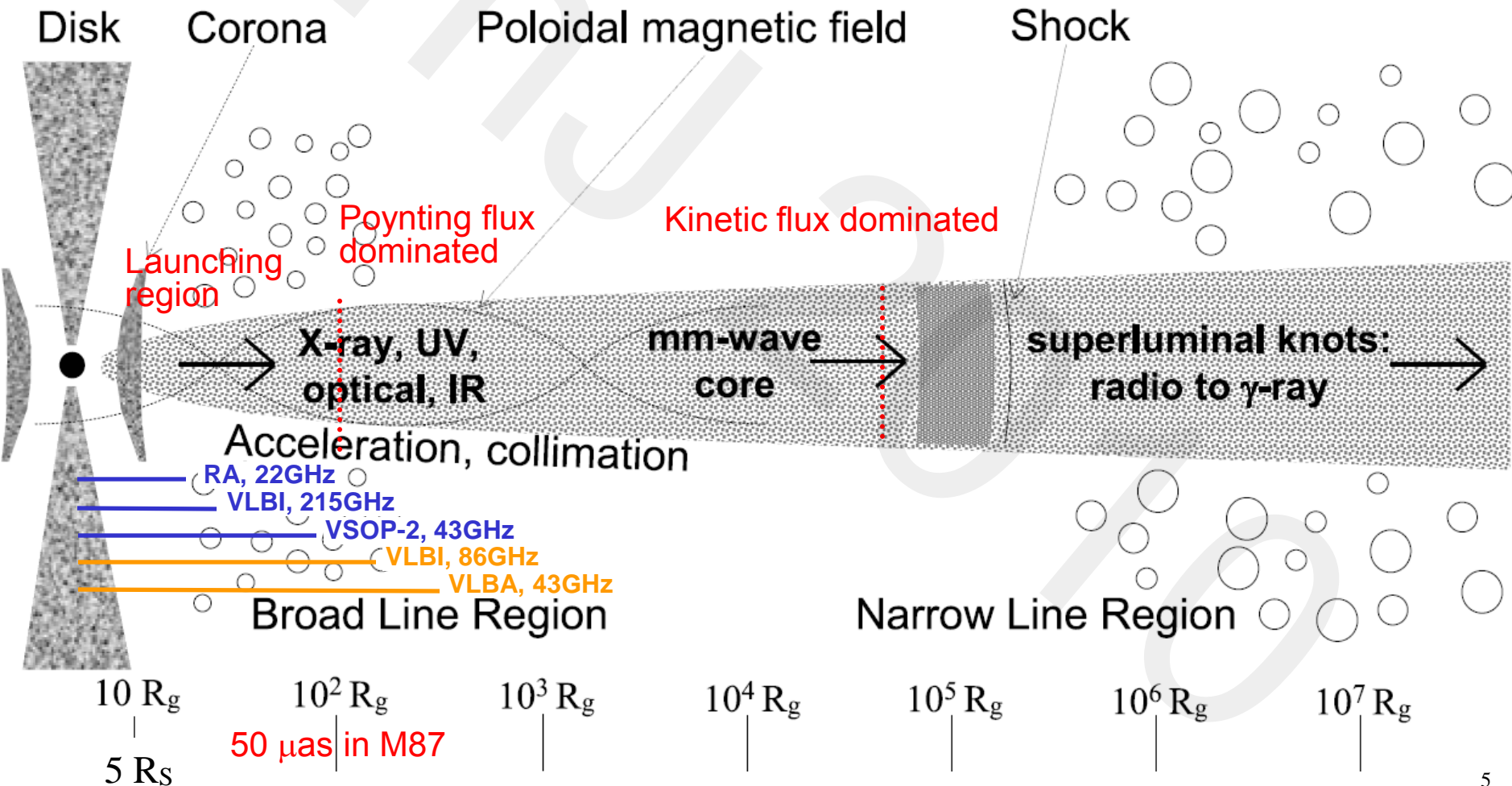
- ❑ Strongly stratified flows.
- ❑ Shocks and CD/KH instability are determining the observed morphological, kinematic and emission properties.
- ❑ Shocks propagate in the faster spine, while instability develops in the outer layers of the flow.





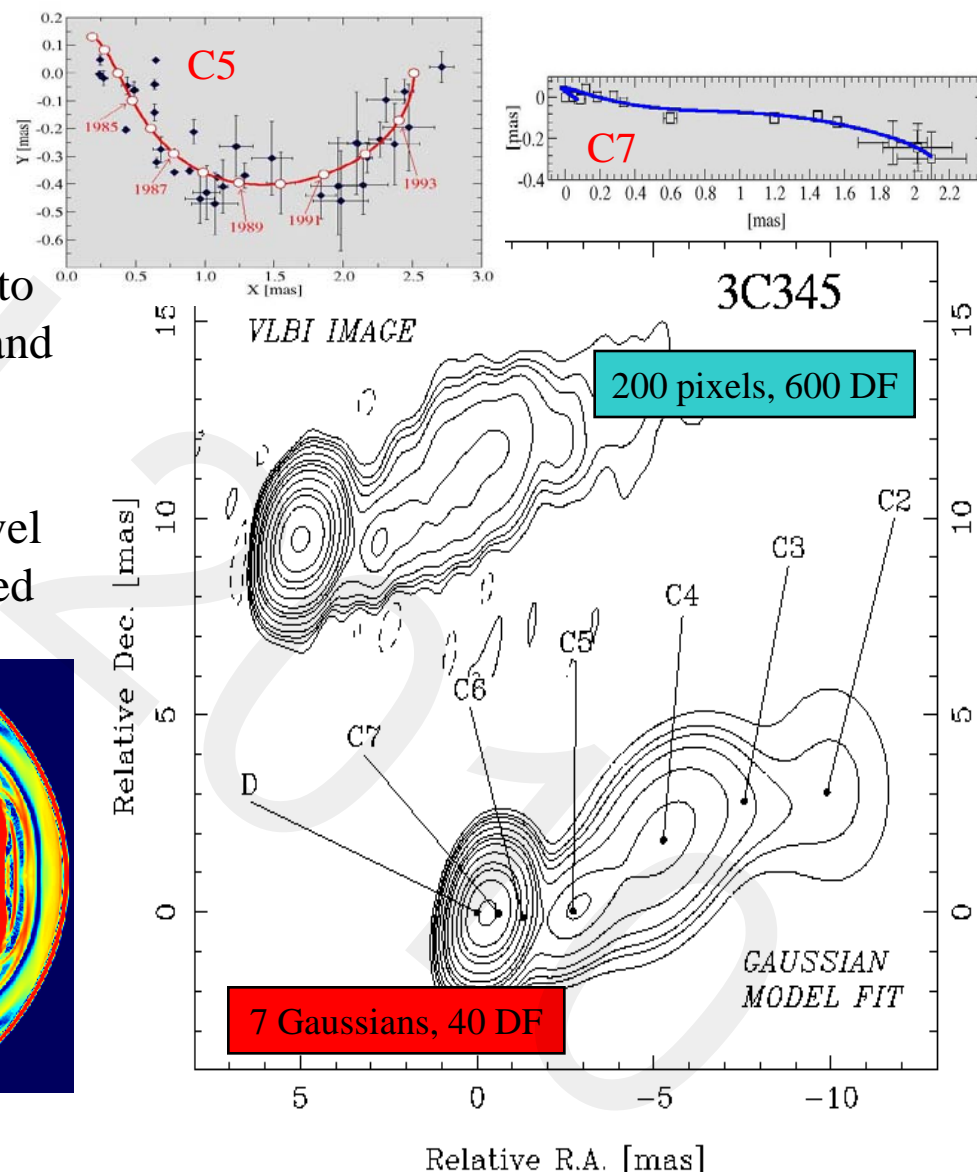
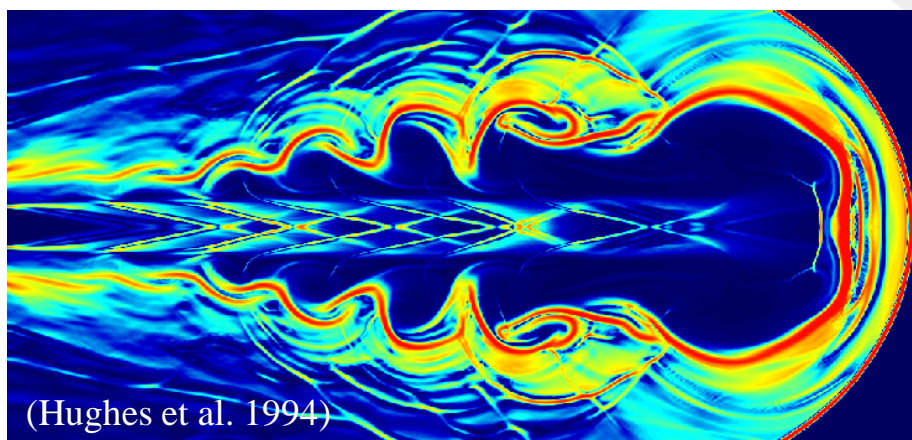
Jets and AGN

- Collimated outflows are formed close to central black holes and they interact with all major constituents of AGN



Information from VLBI

- **Observations:** 1D (routinely), 2D (SoA)
- **Models (relativistic).**
Analytical: 2D (routinely), 3D(t) (SoA)
Numerical: 3D (routinely), 3D(t) (SoA)
- **Problems:** connecting predictions ($\mathbf{p}, \mathbf{v}, \square$) to observables ($\mathbf{S}_{\mathbf{n}}, \mathcal{E}, \delta_{\text{app}}$). Elusive \mathbf{B} , \mathbf{v}_j and \mathbf{M}
- **Solution:** find a way to obtain reliable 2D information from VLBI images. High-resolution and high-fidelity images and novel reduction and analysis techniques are needed

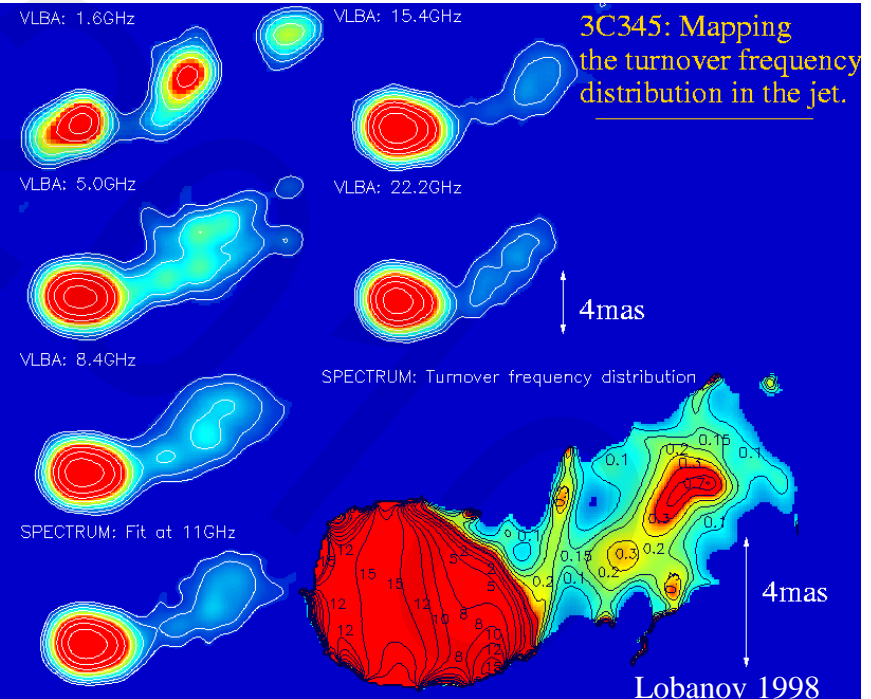
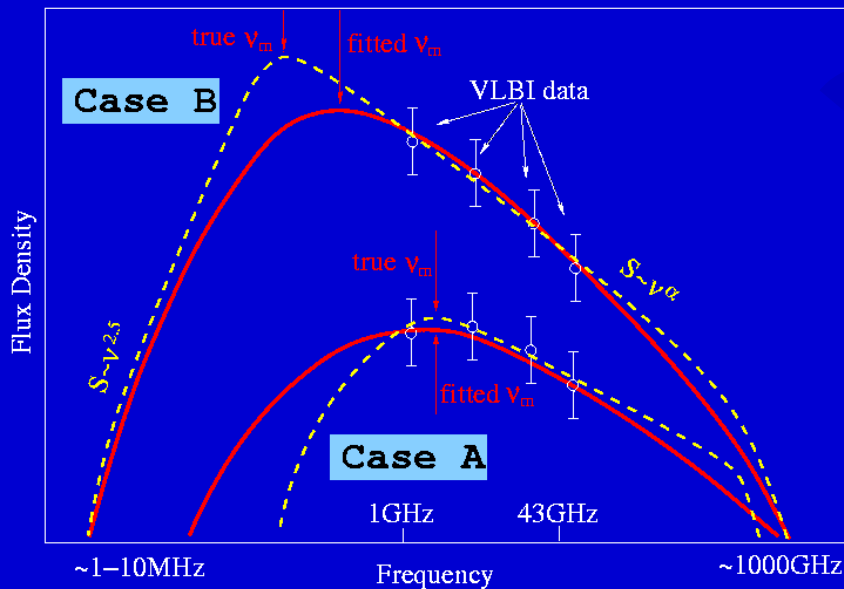




Plasma Diagnostics

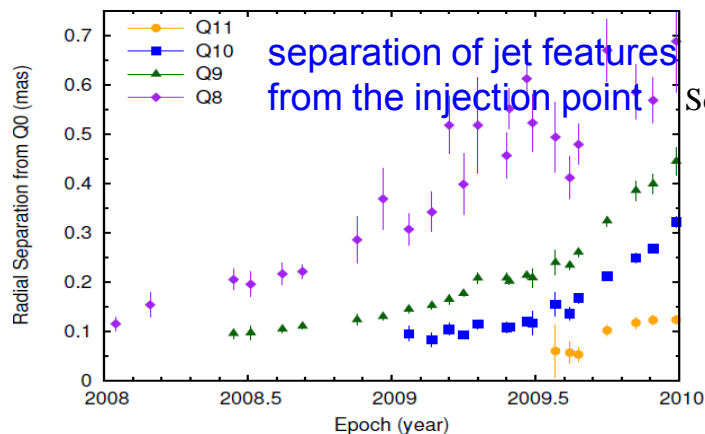
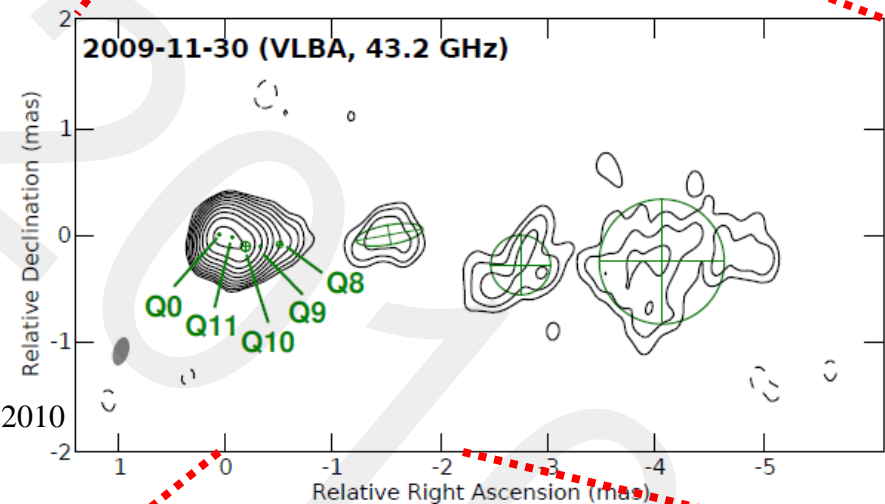
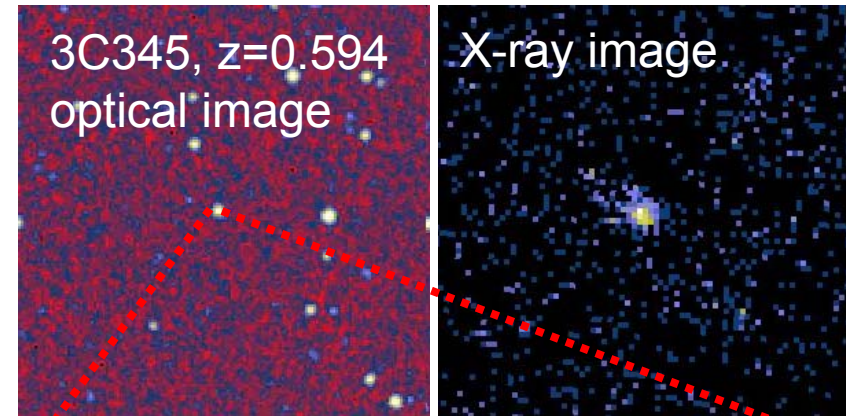
- ❑ Distribution of the spectral turnover: a tool to detect patterns induced by plasma instabilities and obtain two-dimensional distribution of particle density and magnetic field in the flows.
- ❑ Low frequency observations are the only way to enable imaging the spectral turnover in extended jets

Turnover frequency from VLBI data

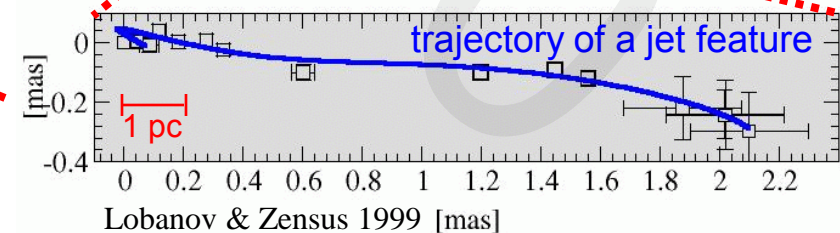


Localisation with VLBI

- VLBI observations now provide a $\sim 50 \mu\text{as}$ resolution at 3 mm, resolving sub-parsec scale regions in all AGN and reaching down to scales of $\sim 100 R_g$ in nearby AGN.
- Monitoring of individual regions traces in detail their kinematic and emission evolution – this evolution can be related to variability of high-energy emission.



Schinzel et al. 2010

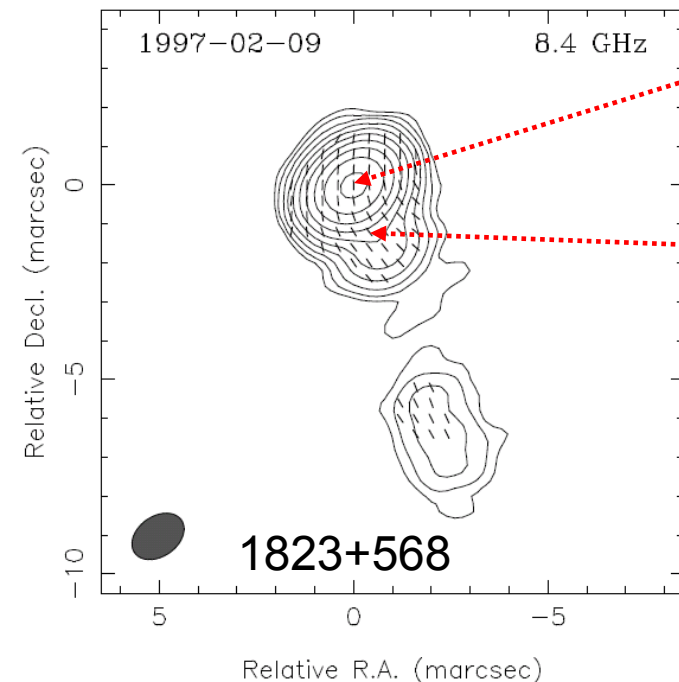


Jet Structure

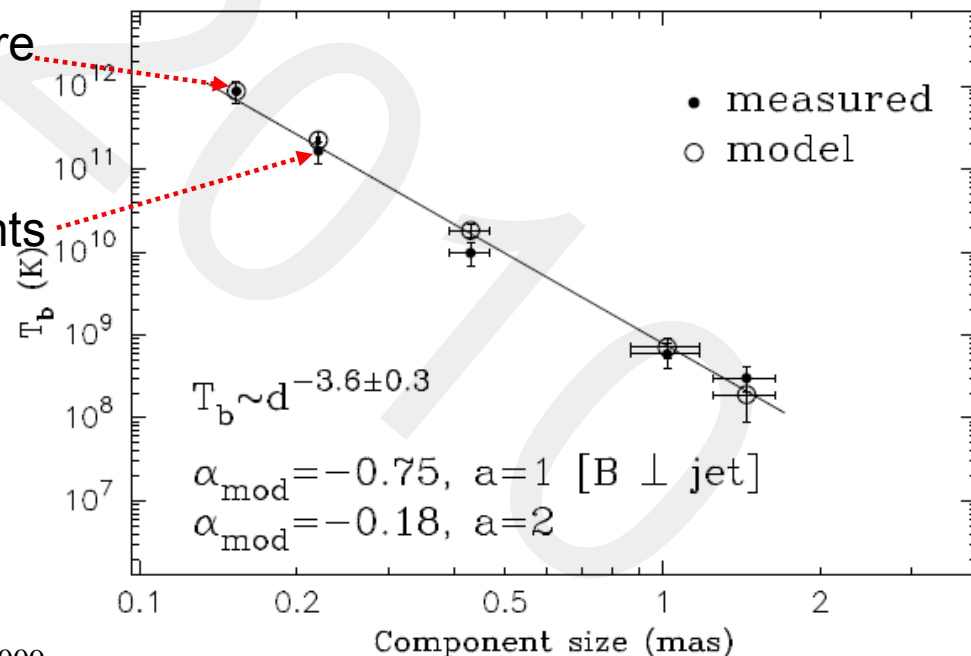


Jet Structure

- ❑ Bright, often unresolved narrow end of the jet (VLBI core), with intrinsic brightness temperature of $\sim 5 \cdot 10^{11} \text{K}$ (Lobanov+2001, Homan+2006).
- ❑ Moving enhanced emission regions (jet components), with intrinsic brightness temperature of $\sim 5 \cdot 10^{10} \text{K}$ (equipartition limit, Readhead 1994) and decreasing in agreement with adiabatic losses (Pushkarev+ 2009).

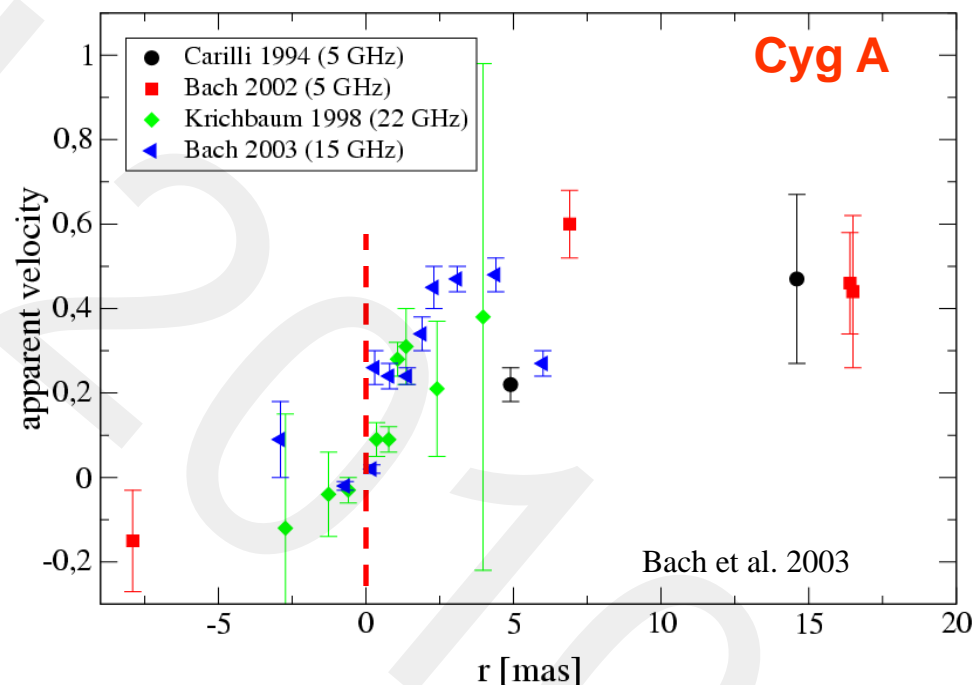
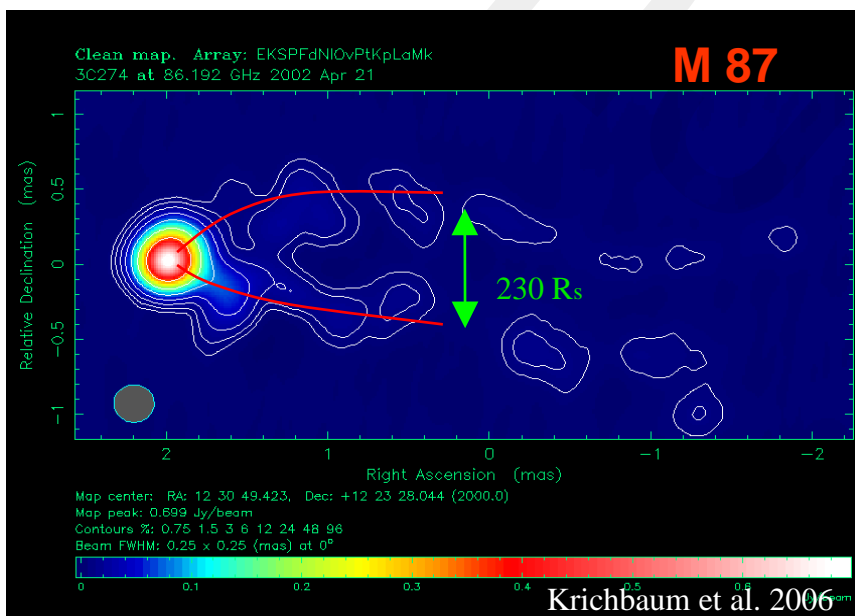


Pushkarev et al. 2009



Collimation and Acceleration

- VLBI observations of compact jets in nearby AGN provide strong evidence for collimation on linear scales of $\sim 10^3 R_g$ and strong acceleration on parsec scales ($\sim 10^5 - 10^6 R_g$)



- Magnetically driven acceleration is a viable explanation for the observed speeds (Vlahakis & Königl 2004)

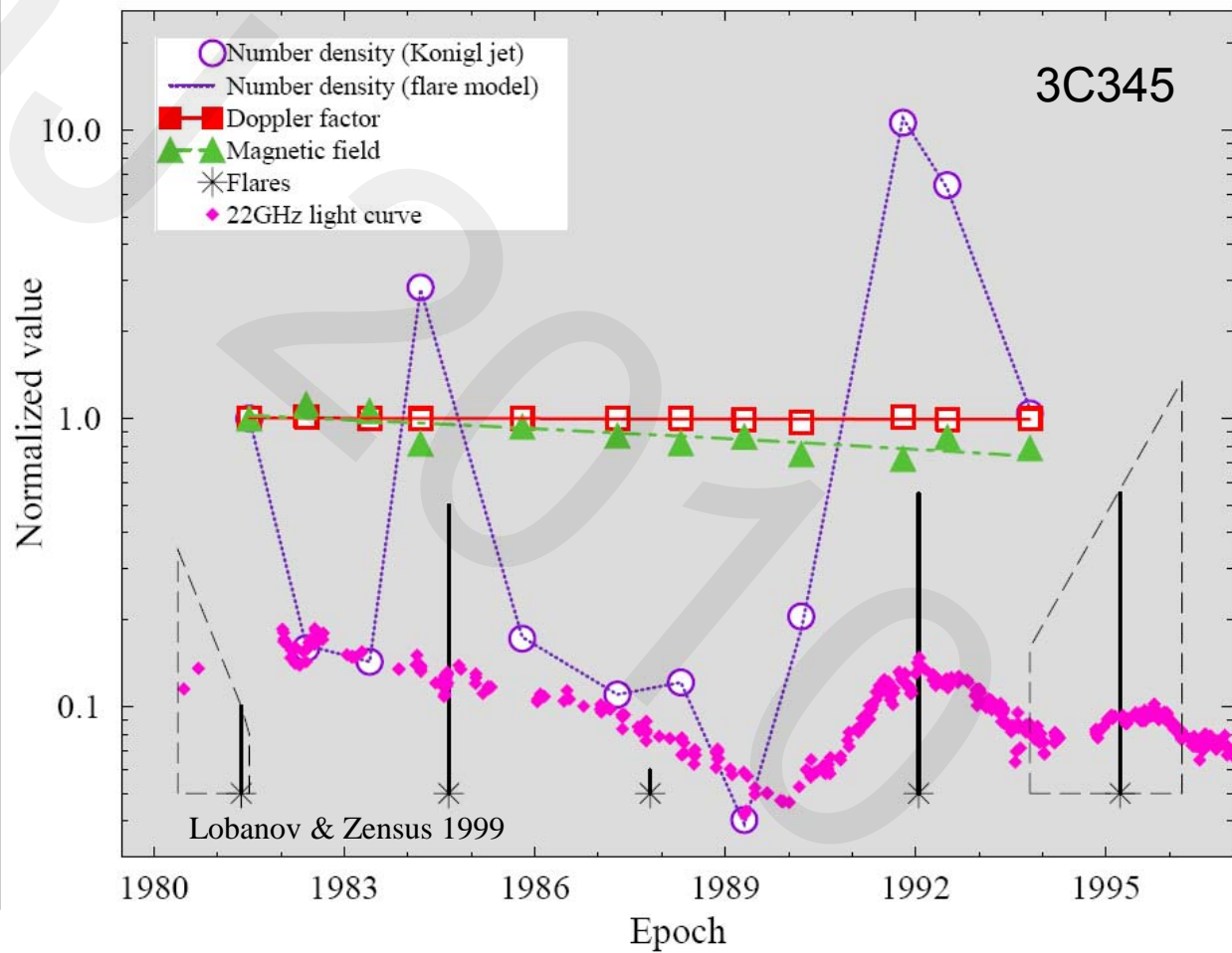
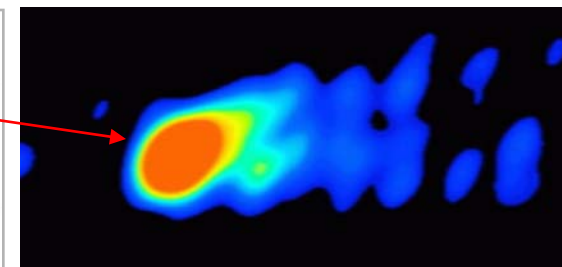
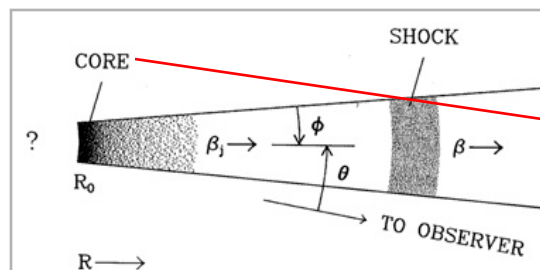


VLBI "Core": Compact Jet

Location at which jets become visible in radio is most likely determined solely by the $\tau=1$ condition for synchrotron emission (Königl 1981).

Nuclear flares can be described by relatively modest and smooth variations of particle density.

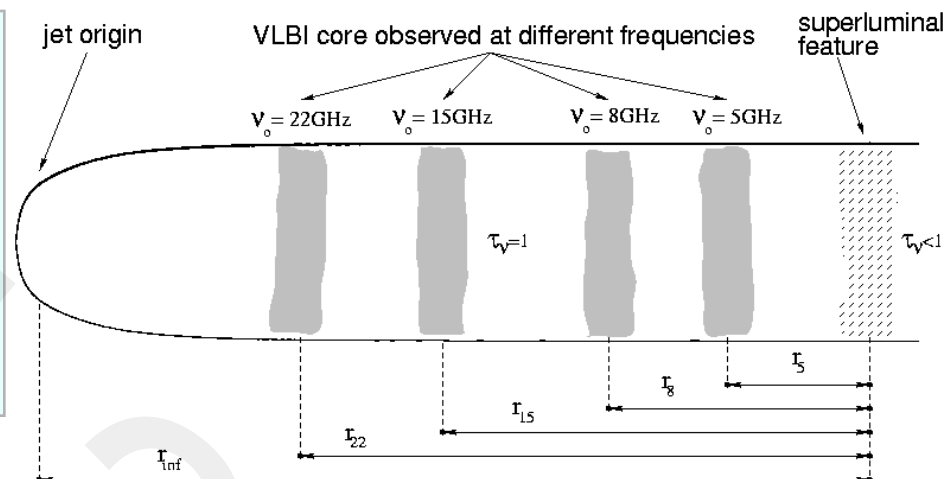
Magnetic fields are either tangled or organized on scales much smaller than the resolution limit.





Ultracompact Jets

❑ Apparent position of the VLBI core depends on observing frequency, owing to synchrotron self-absorption, and external absorption.



Optical depth in the jet

$$\tau_s(r) = C(\alpha) N_1 \left(\frac{e B_1}{2\pi m_e} \right)^\epsilon \frac{\delta^\epsilon \phi_0}{r^{(\epsilon m + n - 1)} \nu^{\epsilon + 1}}$$

The condition $\tau_s = 1$ determines the location of the core

$$r[\text{pc}] = (B_1^{k_b} F / \nu)^{1/k_r}$$

$k_r = 1$ → Synchrotron self-absorption

$k_r > 1$ → Synchrotron self-absorption + Gradients in pressure
 → Synchrotron self-absorption + External absorption (i.e. free-free absorption in the broad-line region)

Can be estimated from observed "core shift"

(Lobanov 1998)



Core Shift

Position offset of the optically thick „core“ of a VLBI jet can be used to estimate physical conditions in the nuclear region of AGN

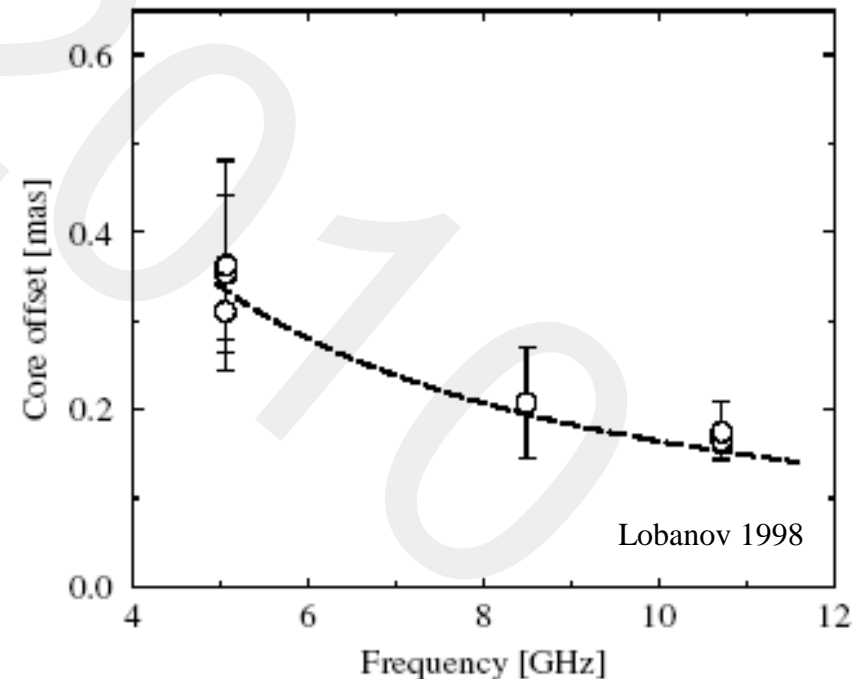
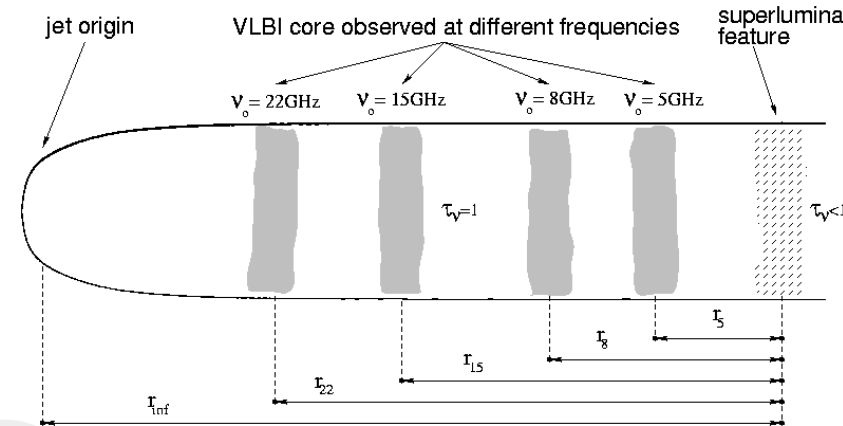
Core offset measure:

$$\Omega_{\tau\nu} = 4.85 \cdot 10^{-9} \frac{\Delta r_{\text{mas}} D_L}{(1+z)^2} \cdot \frac{\nu_1^{1/k_r} \nu_2^{1/k_r}}{\nu_2^{1/k_r} - \nu_1^{1/k_r}}$$

Derived magnetic field and distance from the central engine to the core:

$$B_1 = (\Omega_{\tau\nu} / \sin \theta)^{k_r/k_b} F^{-1/k_b}$$

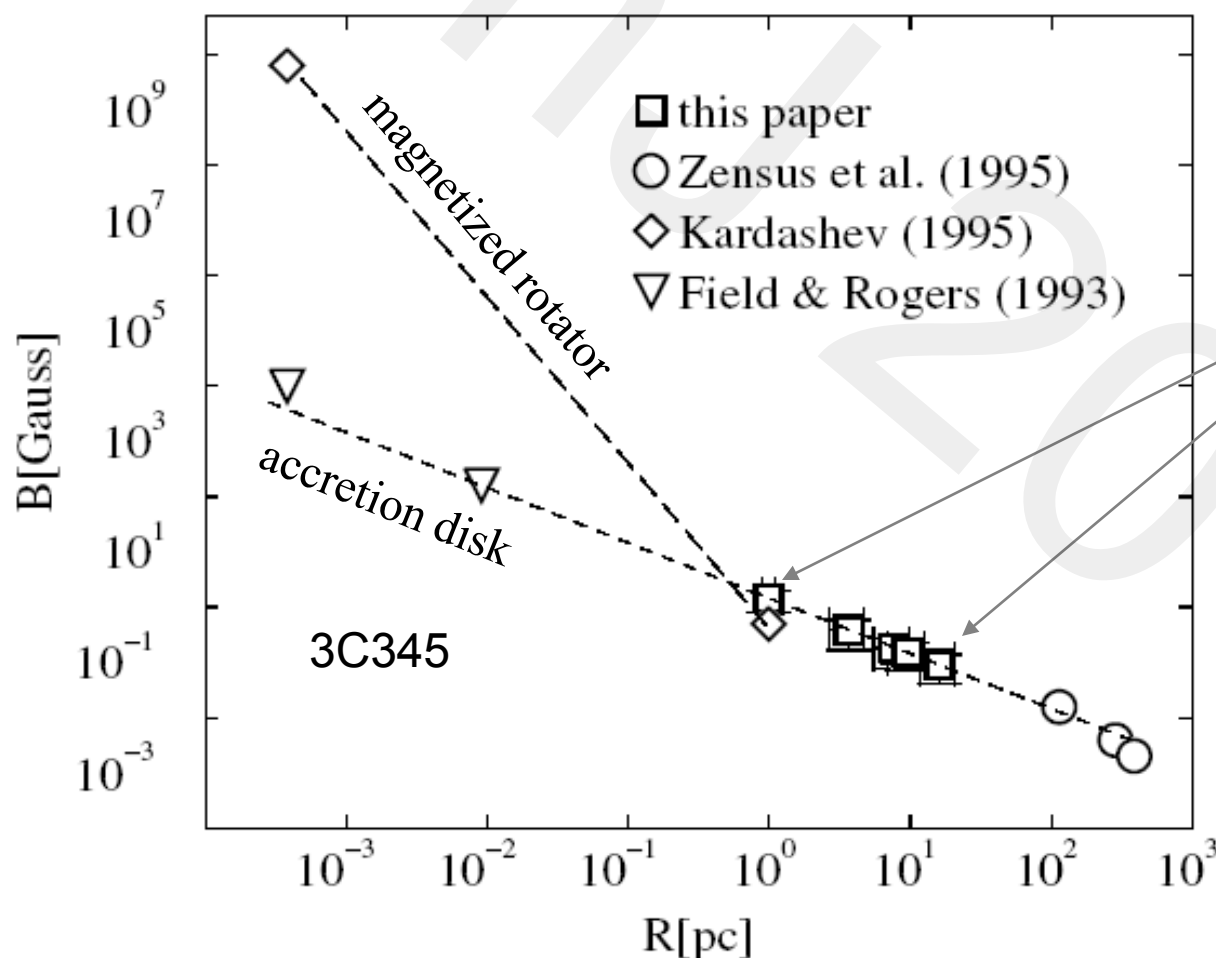
$$r_{\text{core}}(\nu) = \Omega_{\tau\nu} \left[\nu^{1/k_r} \sin \theta \right]^{-1}$$





Magnetic Field near SMBH

- Multifrequency measurements of the core shift in 3C345 enable determining properties of the magnetic field on parsec-scales in the jet of this object.



Measured from the core shift

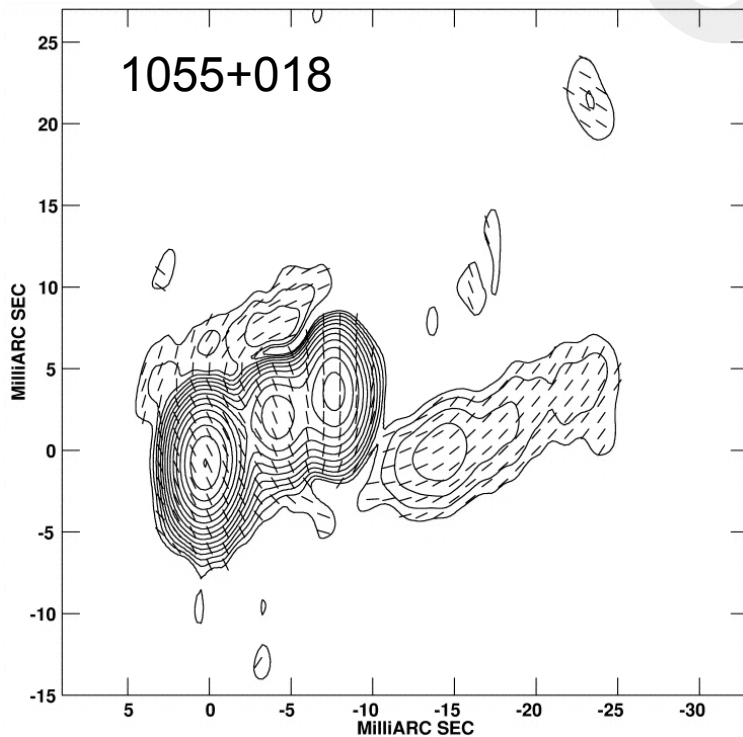
Typical fields of order of $\sim 1\text{G}$ in VLBI cores and less than 0.1G in jet components

– see presentation by Kirill Sokolovsky.

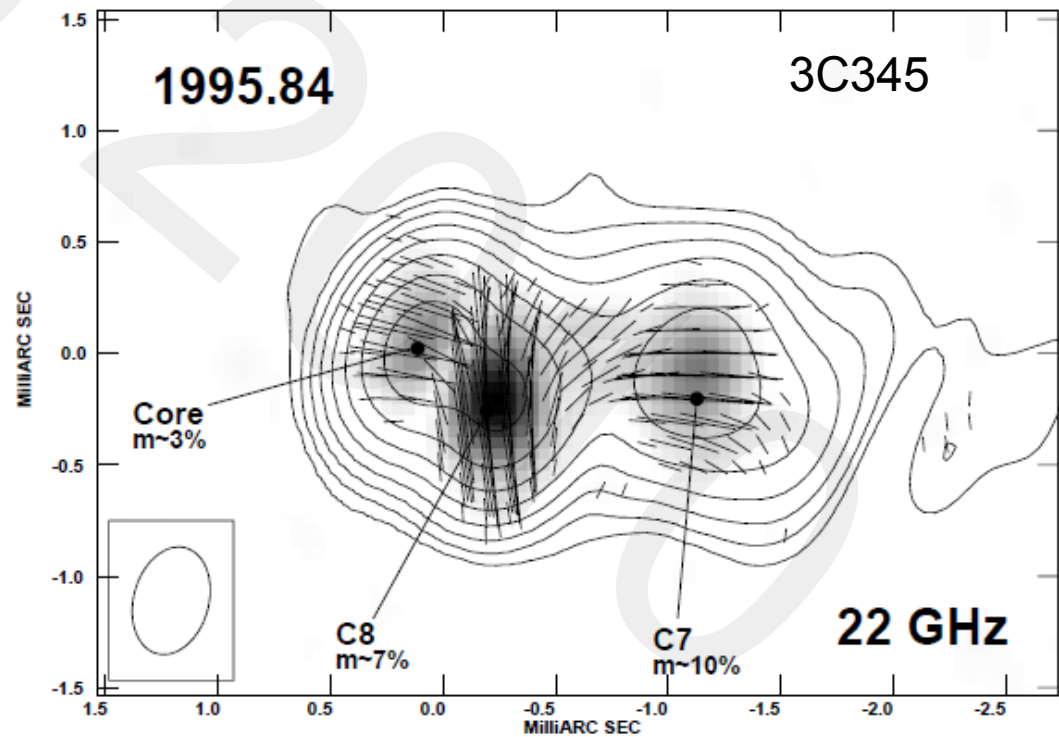


Magnetic Field Structure

- ❑ Jet spine: poloidal field + shock compressed regions. Presence of helical magnetic field is also suggested from EVPA rotation and rotation measure gradients.
- ❑ Outer layers: toroidal field + shear stretched regions.



Attridge et al. 1999



Ros et al. 2000

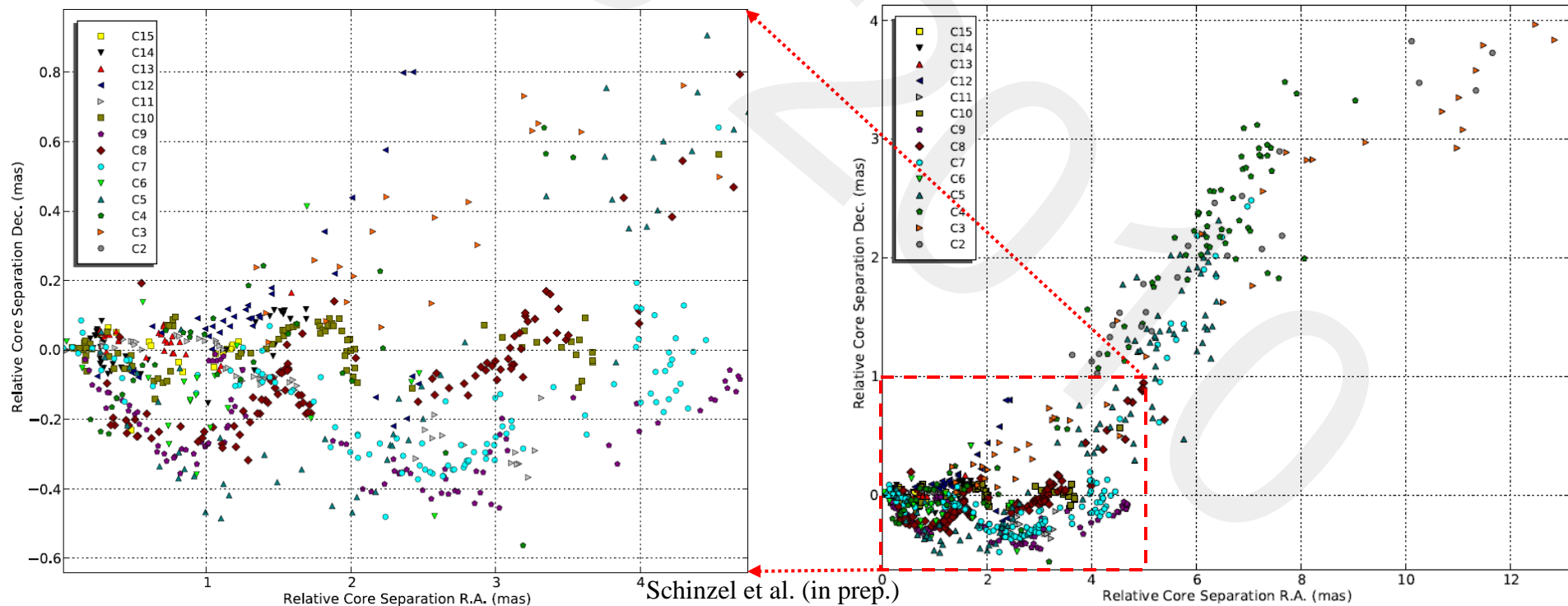
Kinematics



Component Trajectories

- ❑ Trajectories of individual jet components often differ substantially in the vicinity of the VLBI core, but later align well with the general direction of the jet.
- ❑ Filaments inside a straight flow? Rotating flow? Strongly dominating magnetic field?

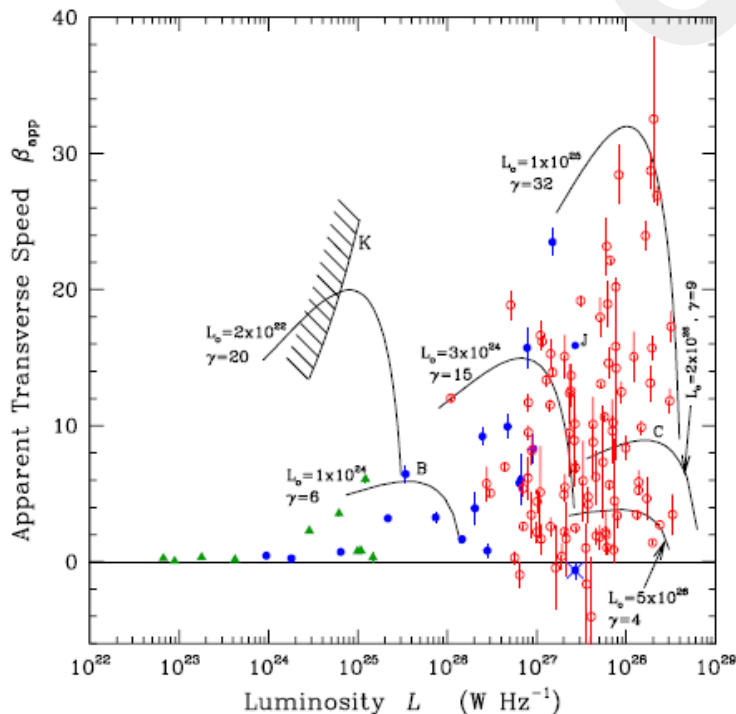
positions of jet components in 3C345



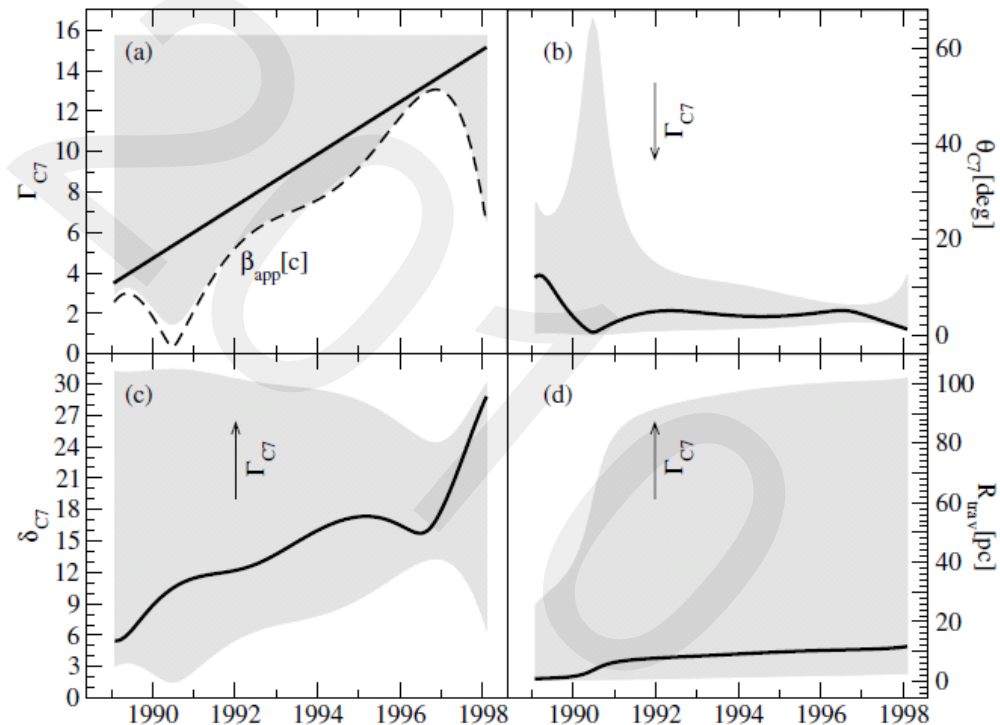


Proper motions

- ❑ Proper motions reflect underlying flow speed (Lister+2009). An envelope with $\Gamma_j \sim 30$, possibly varying in different source types.
- ❑ Accelerated motions are common, as well as presence of quasi-stationary regions (Homan+2006)
- ❑ Rest frame acceleration is likely, with acceleration scales of ~ 10 pc.



Cohen et al. 2006

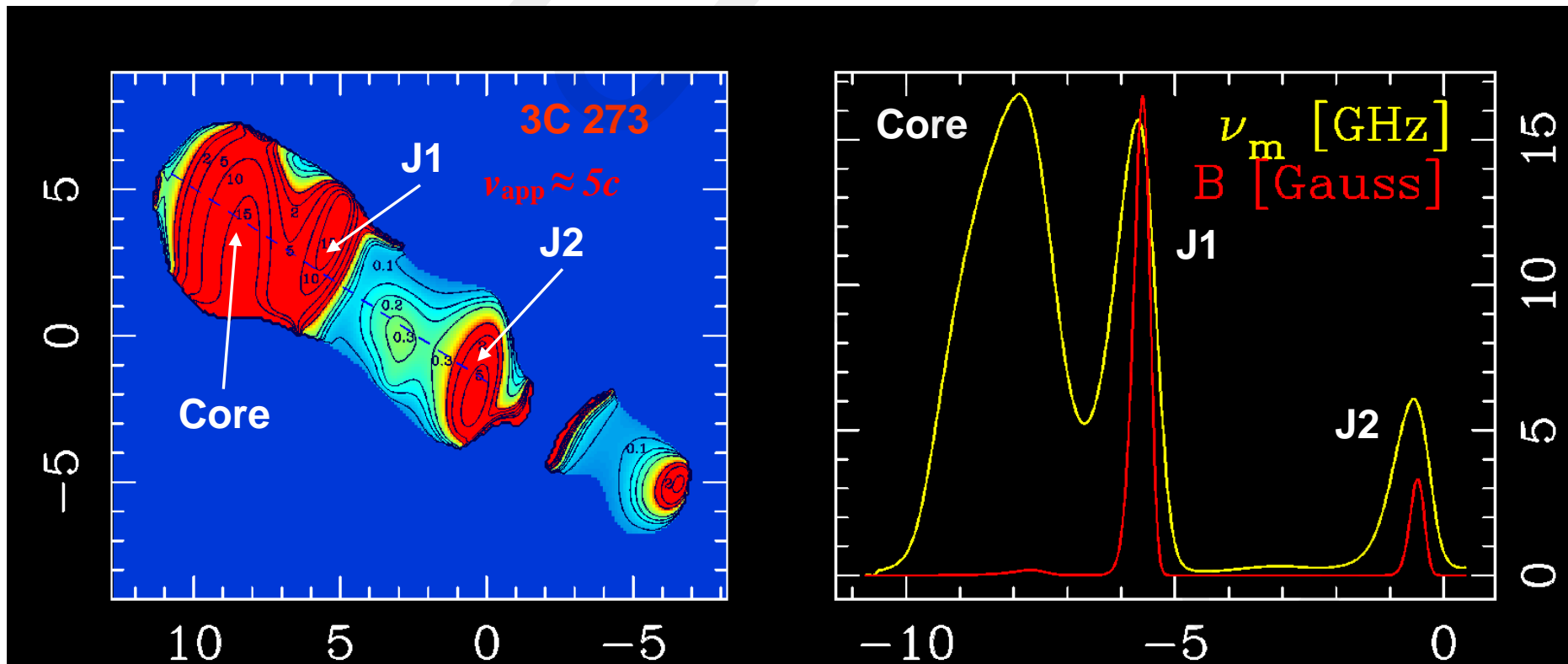


Lobanov & Roland 2005

Shocks and Plasma Instability

Shock-Dominated Regions

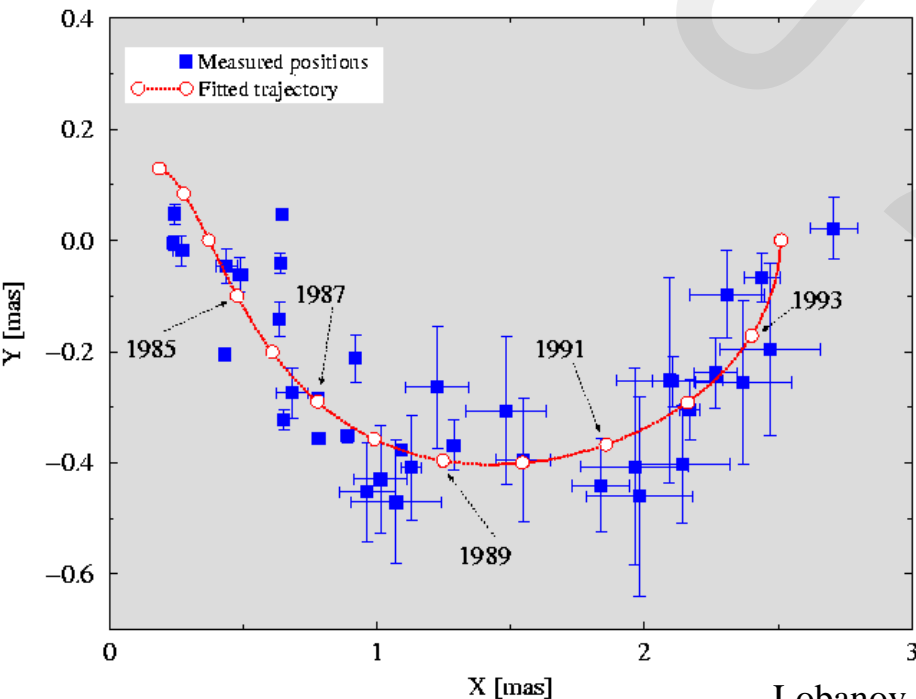
- Strong shocks are present in jets on scales of several decaparsecs ($10^6 - 10^7 R_g$) – revealed by polarization of radio emission and distribution of the synchrotron peak frequency.



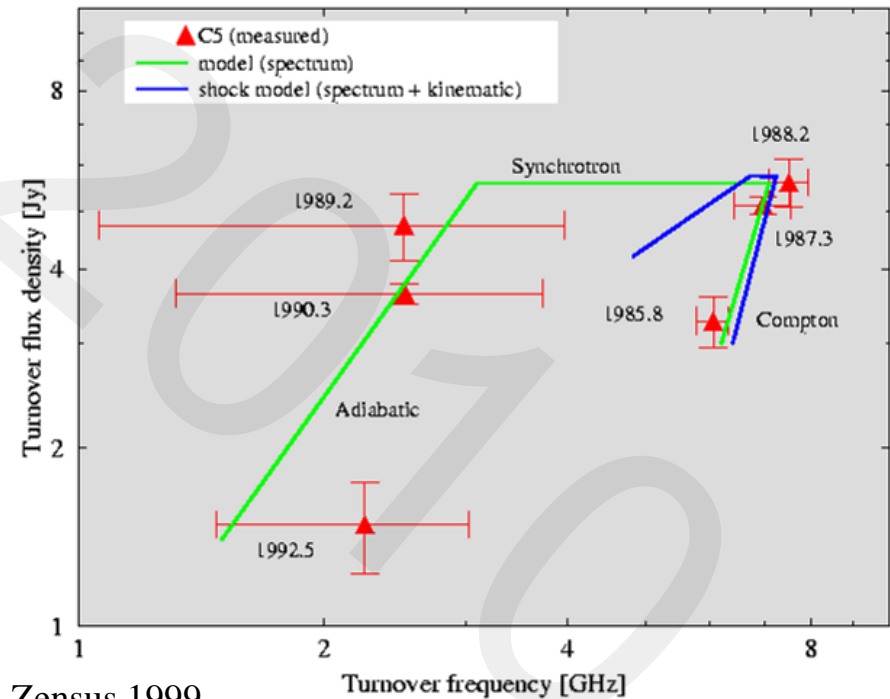


Shocks on parsec scales

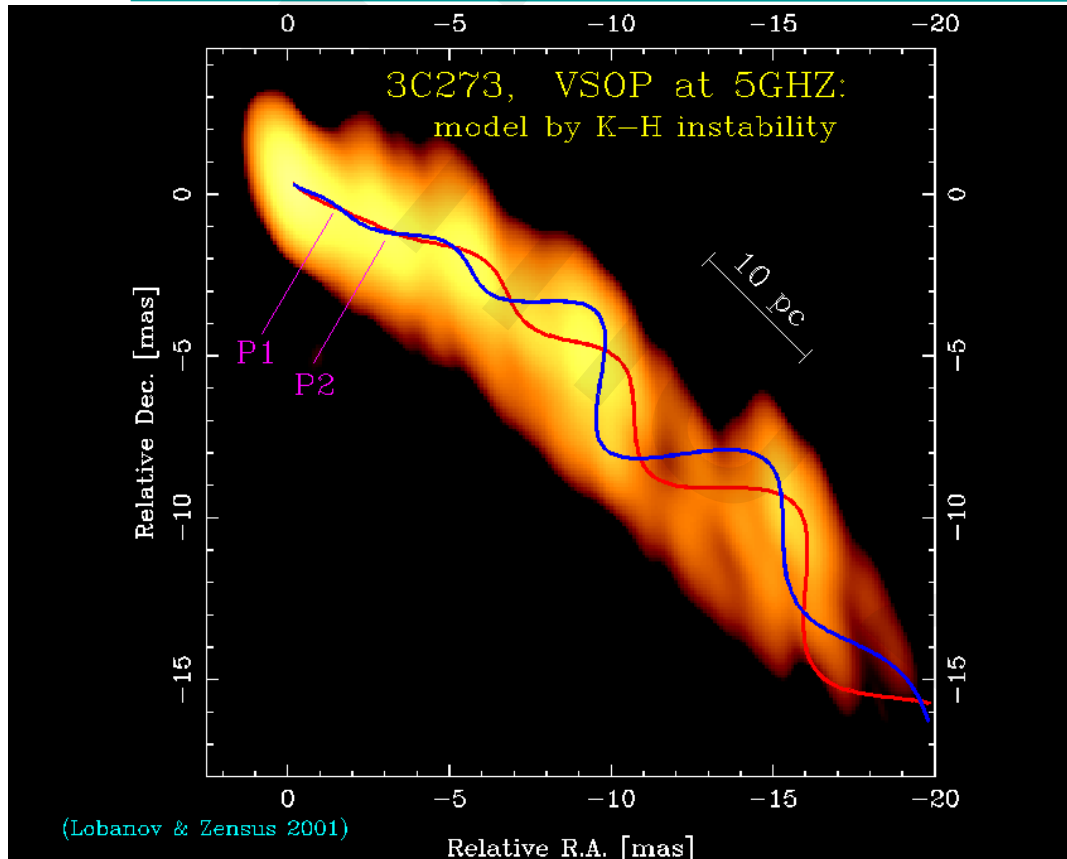
- Shocks dissipate rapidly while approaching hectoparsec scales: shock models can no longer explain kinematic and spectral evolution observed in jets on these scales.

3C345: trajectory of C5


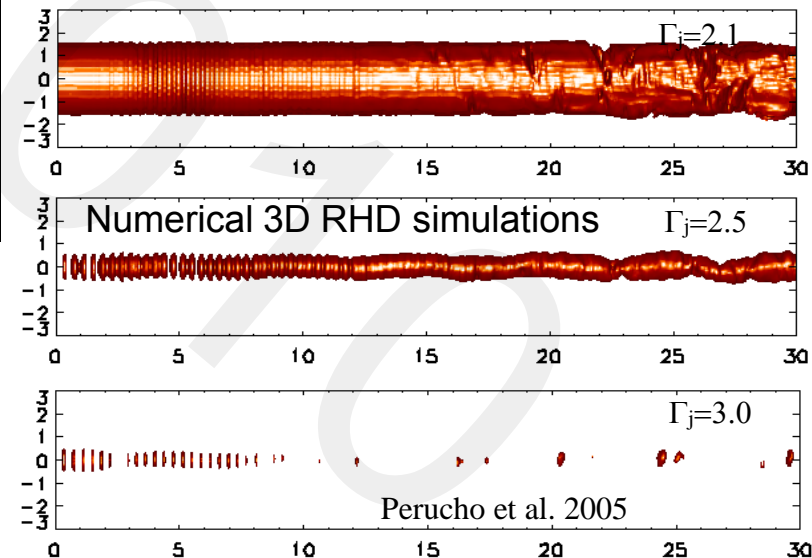
Lobanov & Zensus 1999

Turnover frequency evolution in C5 (3C345)


Shocks and K-H Instability



- Shocks dissipate at distances of $>10^7 R_g$, giving way to Kelvin-Helmholtz instability as the major factor determining the morphology and dynamics of the flow. The instability develops in a non-linear regime



Wavelengths of the modes:

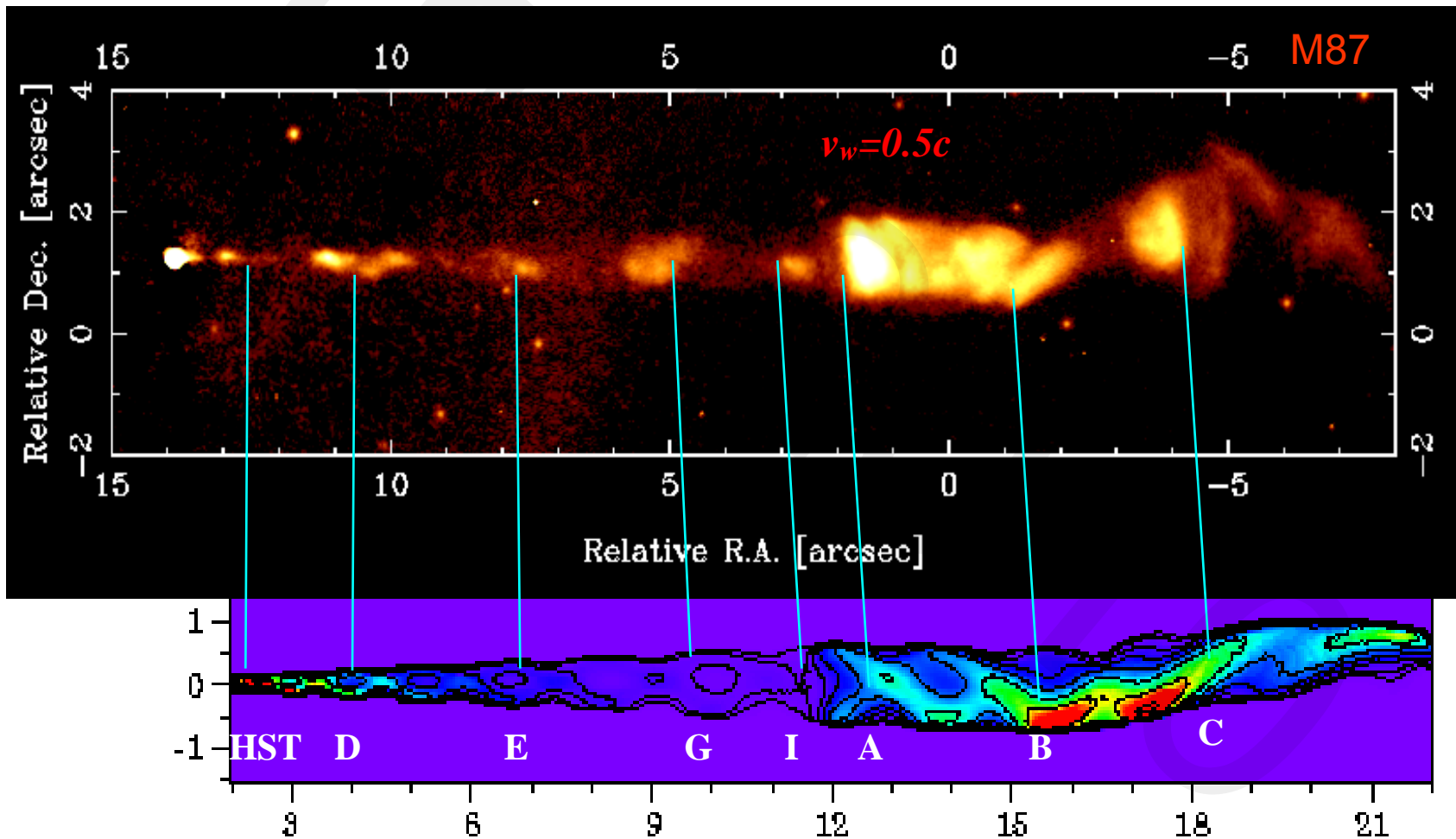
$$\lambda_{\text{HS}}=18.0, \lambda_{\text{ES}}=12.0, \lambda_{\text{Eb1}}=4.0, \lambda_{\text{Eb2}}=1.9 \text{ [mas]}$$

Jet parameters:

$$G_j=2.1, M_j=3.5, \eta=0.02, a_j=0.53, v_w=0.21c$$

Instabilities on Large Scales

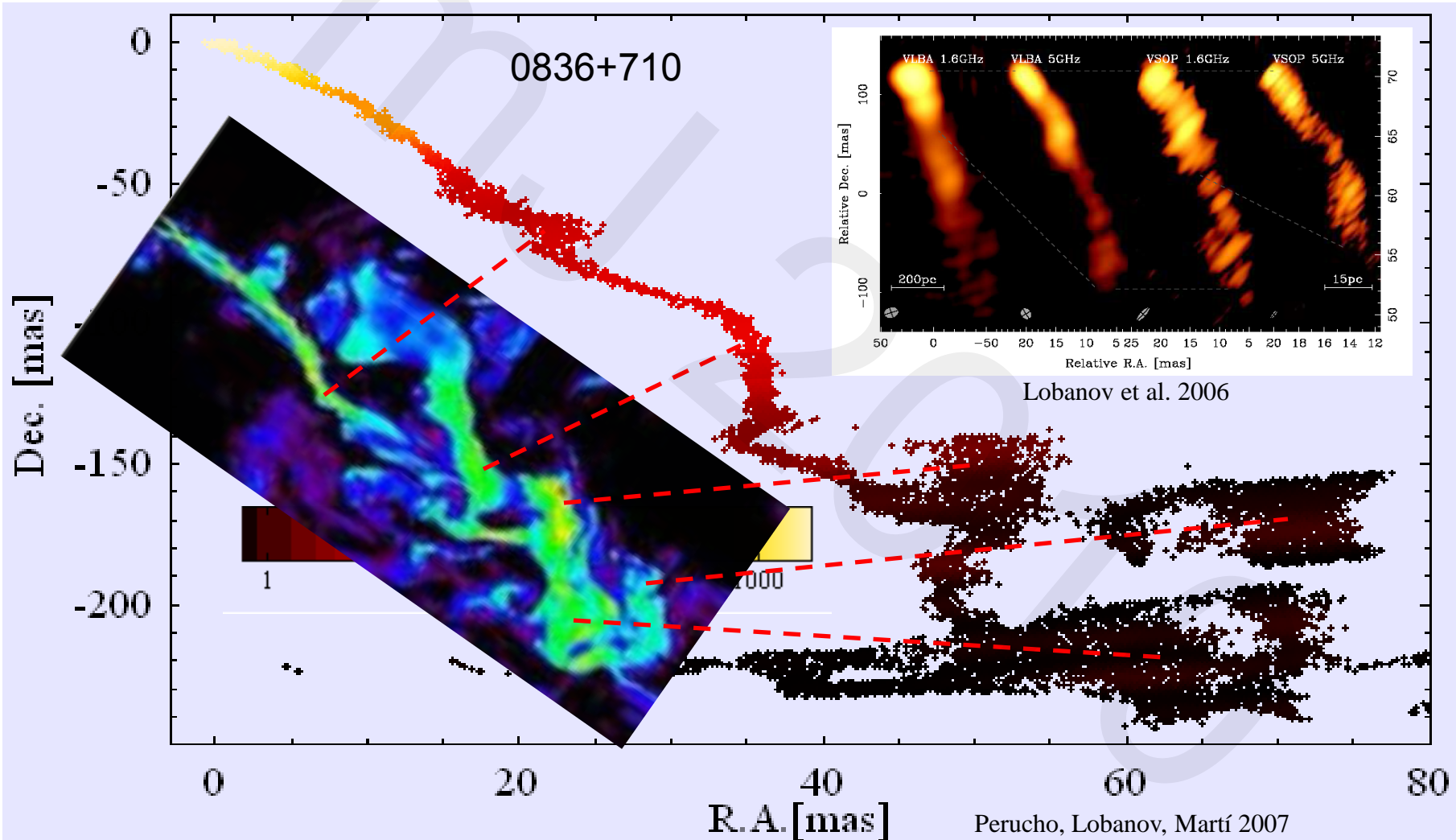
- Kelvin-Helmholtz instability determine the morphology and dynamics of jets on scales of $10^7 - 10^9 R_g$





Jet Disruption

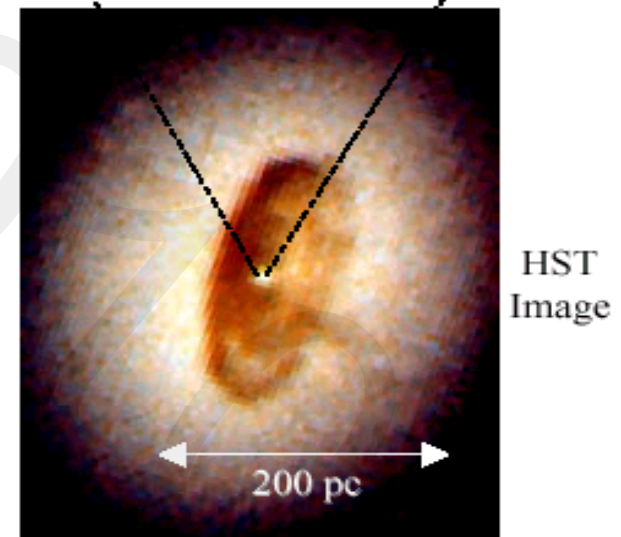
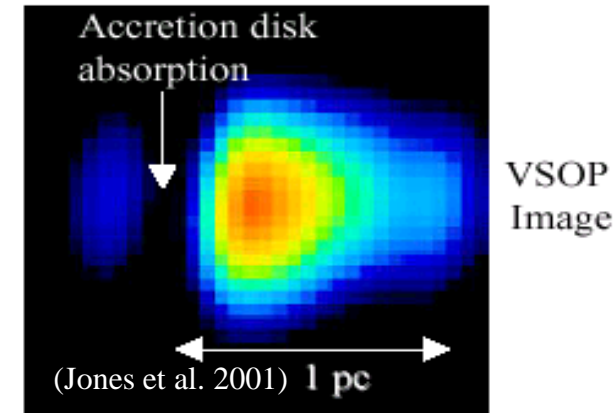
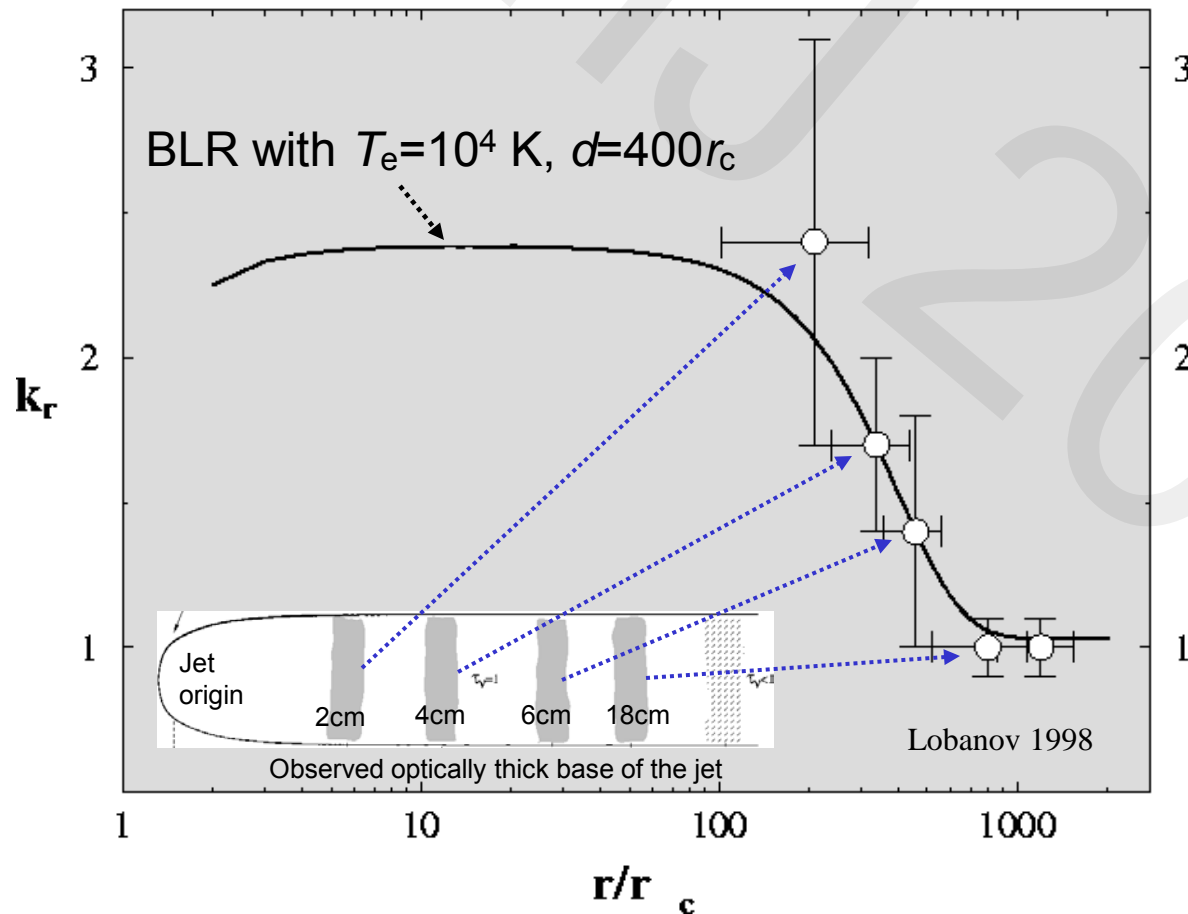
- Helical surface mode of K-H instability can disrupt jets at $\sim 10^9 - 10^{10} R_g$



Broad-band Continuum

- ☐ Nuclear absorption studies of radio emission from jets probe accretion disks and broad-line regions in AGN

3C309.1: opacity in the jet

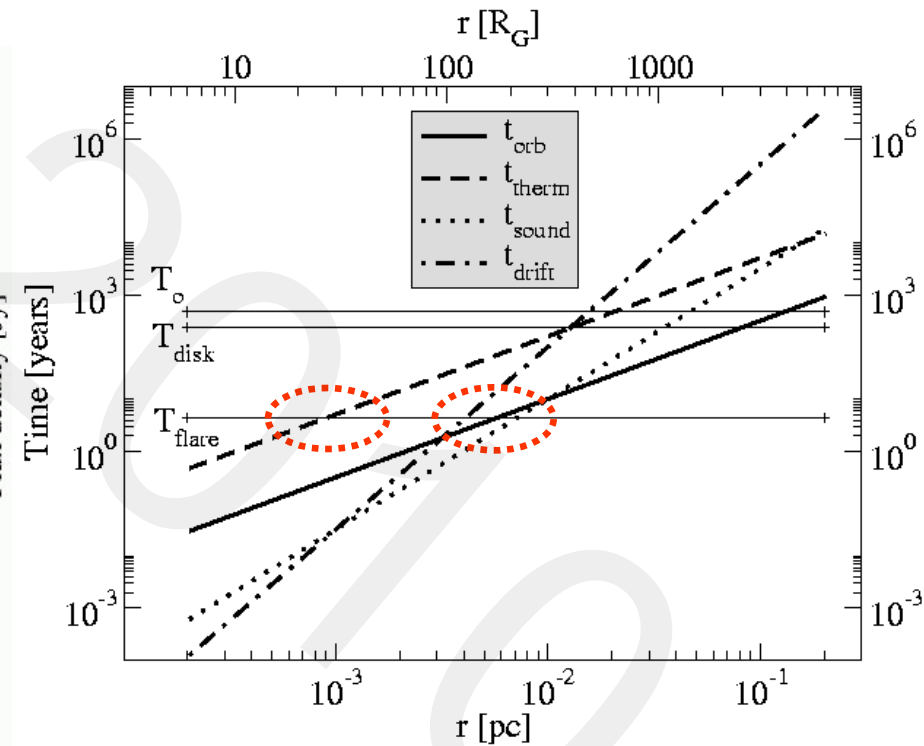
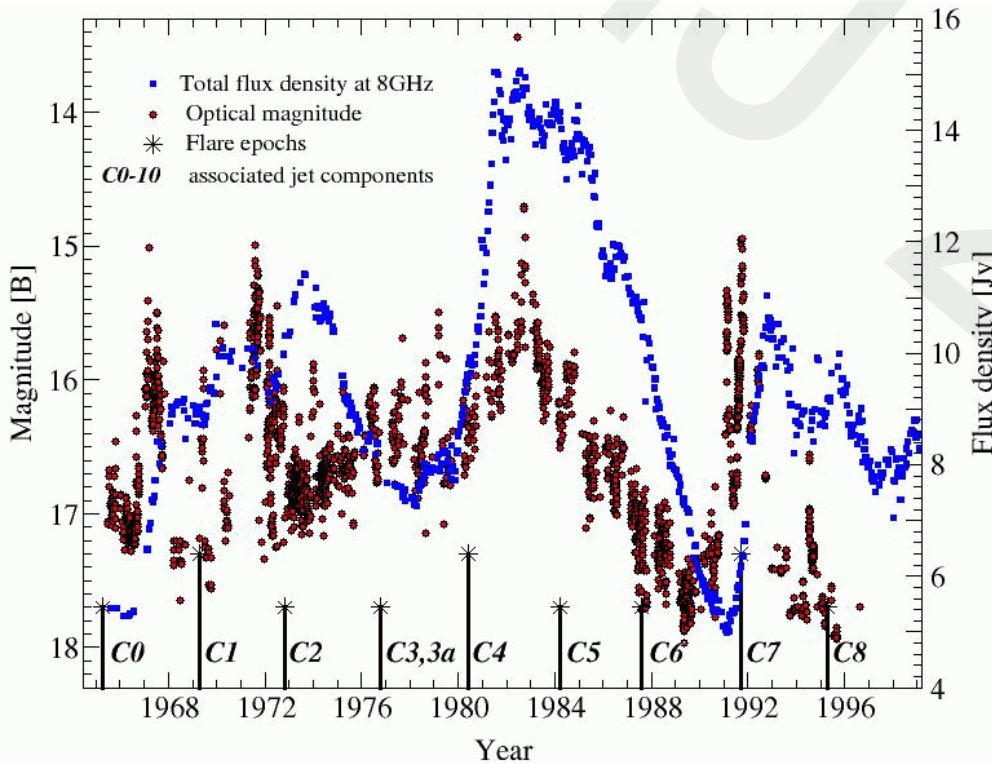


Accretion Disk in NGC 4261



Jet-Disk Connection

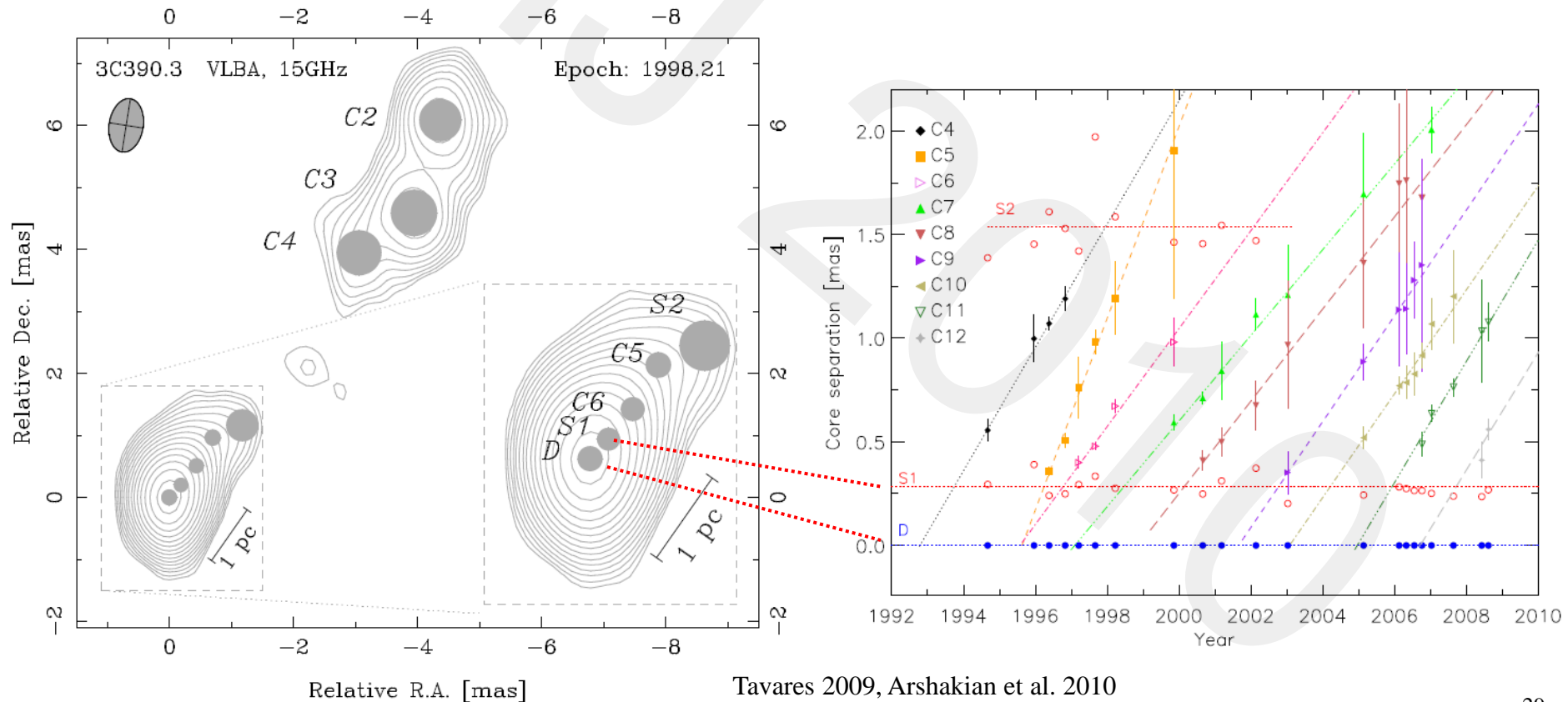
- Flares and ejections of new jet components in 3C345 may be related to the characteristic instability timescales in the accretion disk at 20-200 R_g





Is Jet Influencing BLR?

- Using VLBI observations to relate structural changes in the jet to optical variability in 3C390.3
- Linear fits to component separations yield epochs of ejection from the central engine D and passages through the stationary region S1





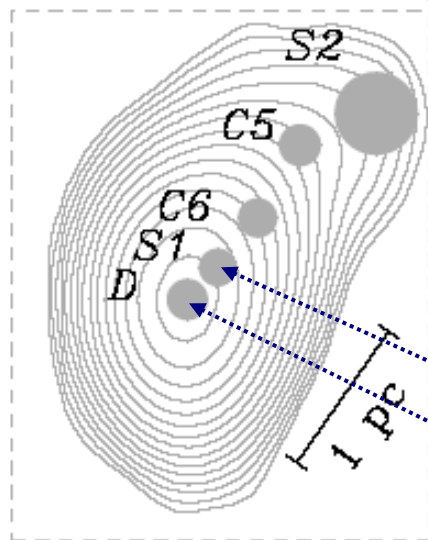
Jet Optical Continuum

- Two different line components in broad-line emission in 3C390.3 and are driven by two different continuum radiation sources located near the accretion disk (D) and in the jet (S1). S1 is a stationary formation (possibly a recollimation shock or acceleration end zone).

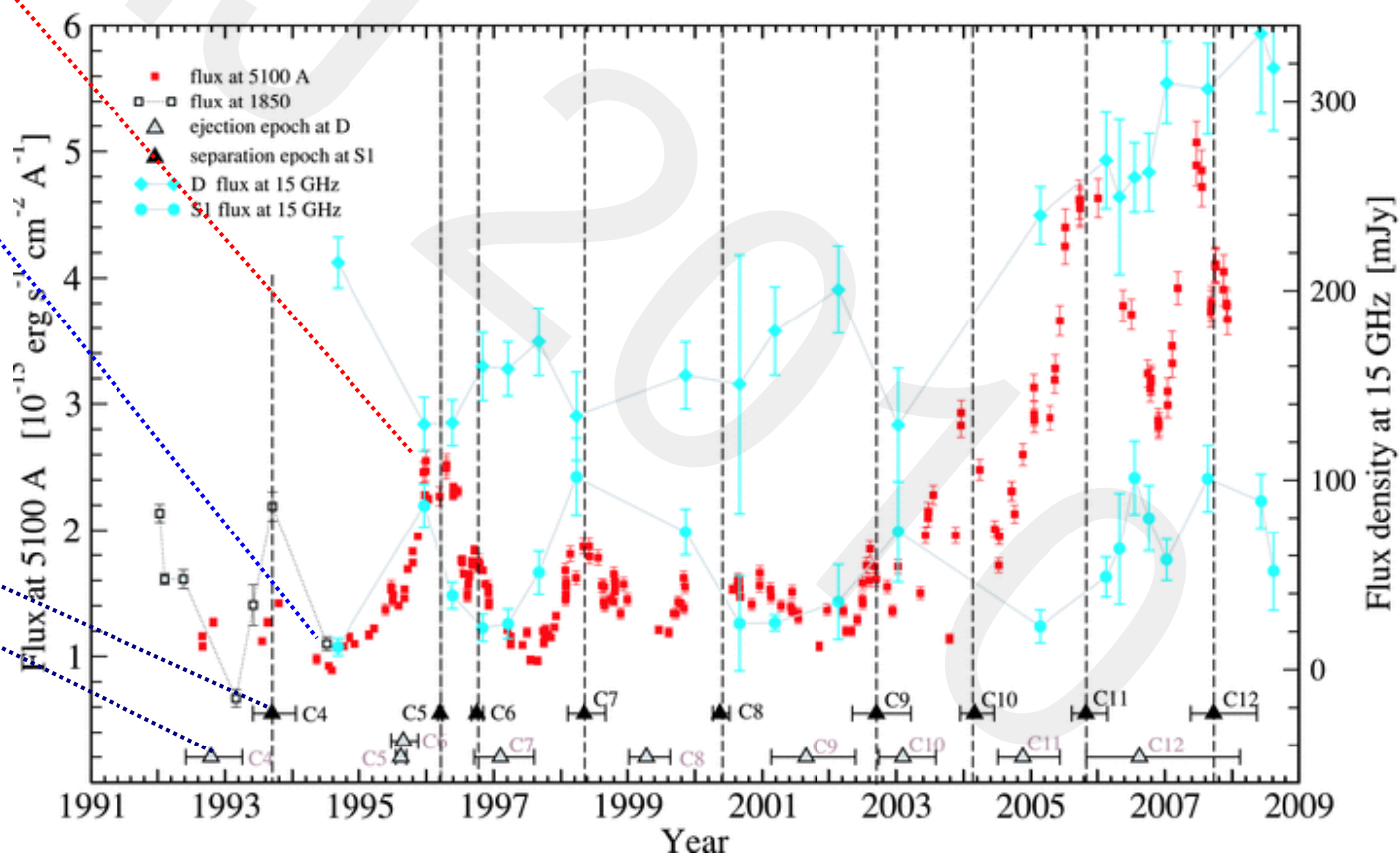
$$W_{H\beta} = 10000, 12000 \text{ km/s}$$

$$\tau_{\text{cont-line}} = 30, 100 \text{ days}$$

$$M_{\text{bh}} = 4 \times 10^8 M_{\text{sol}}, 2 \times 10^9 M_{\text{sol}}$$



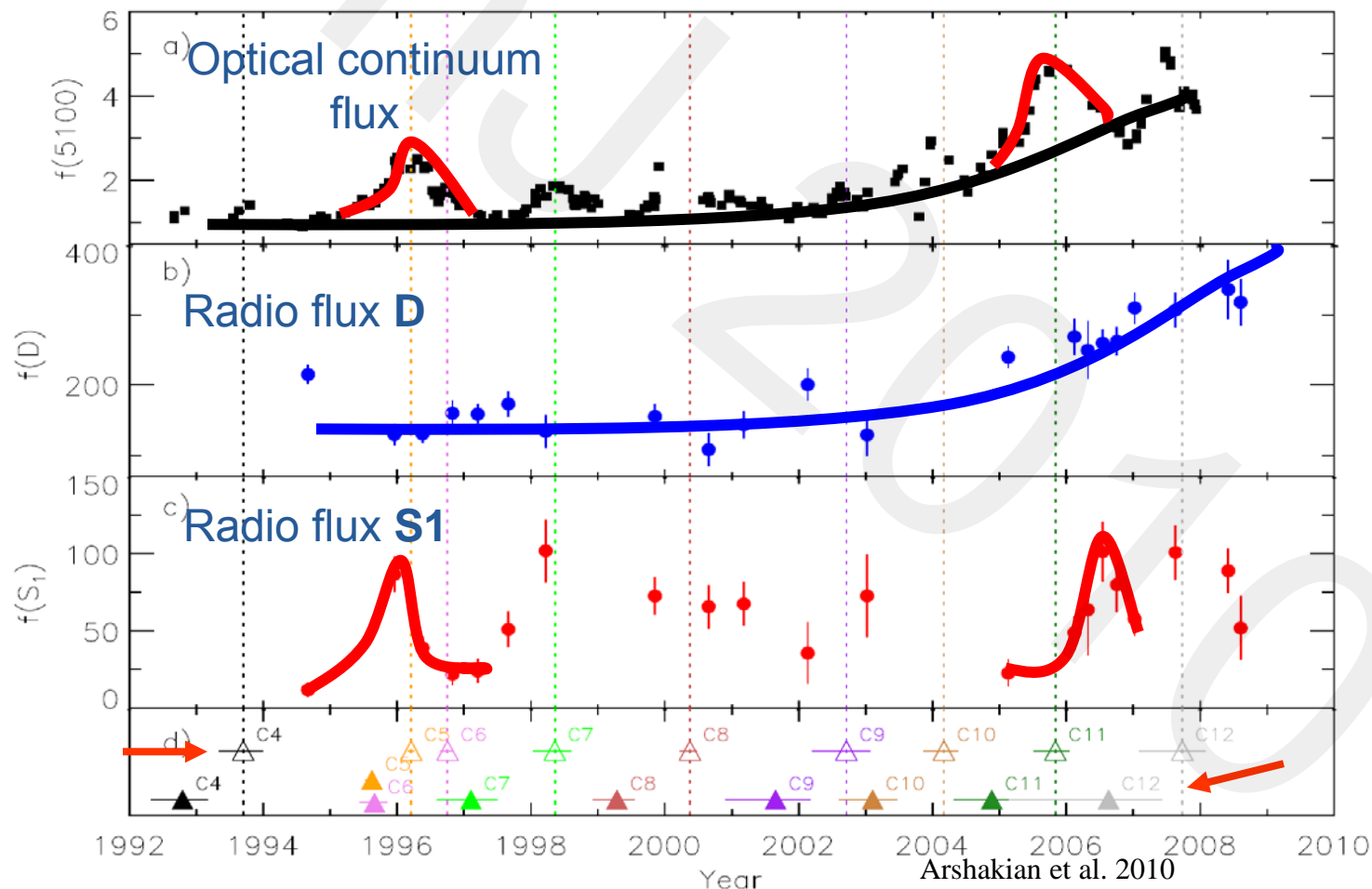
Arshakian et al. 2010





Optical and Radio Variability

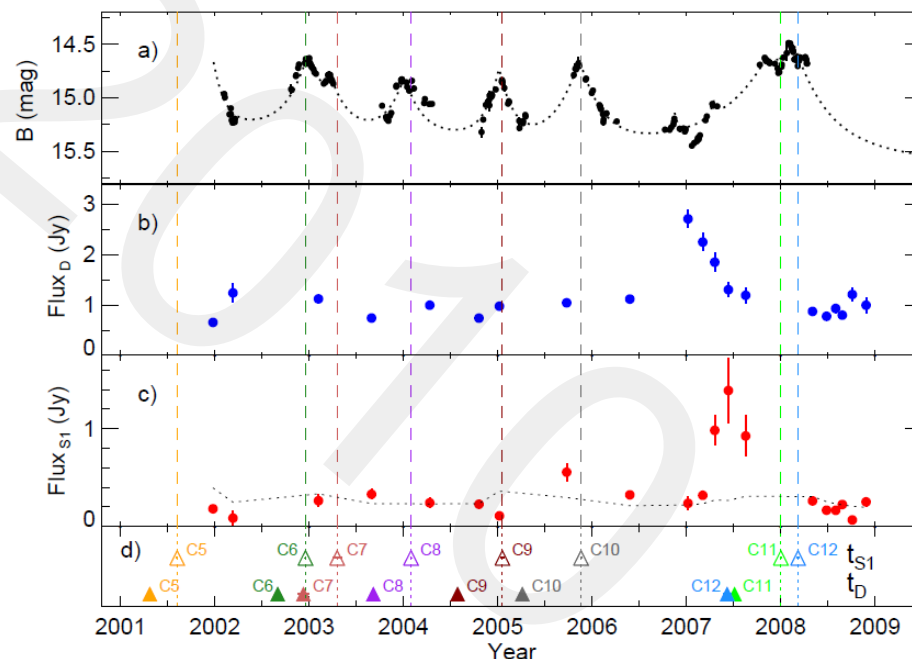
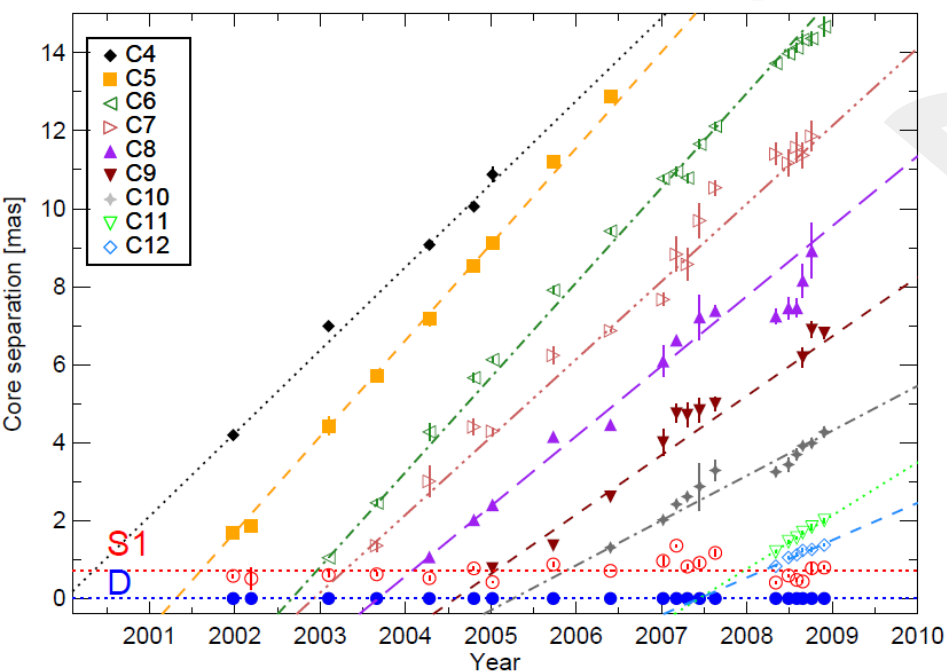
- Flaring component of the optical continuum is associated with the stationary region S1 located in the jet, at a ~ 1.3 pc distance from the putative central engine of 3C390.3





The Case of 3C120

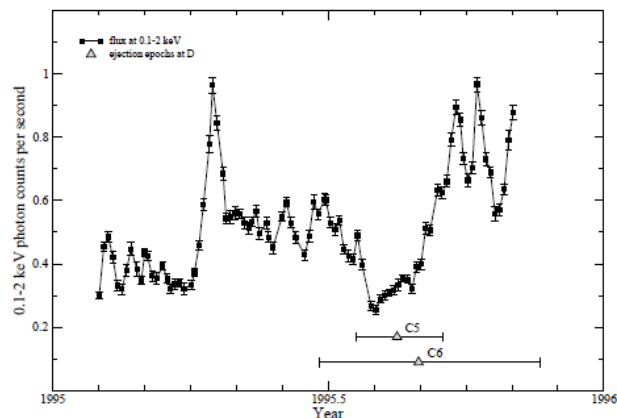
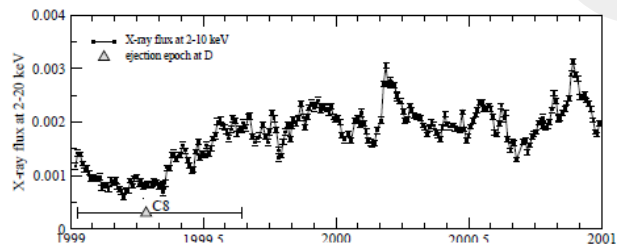
- ❑ 3C120: The same relation between optical flares and passages of jet components through a stationary region located at about 1 pc from the jet origin.
- ❑ VLBI data are too sparse to make any conclusions about variability of radio emission. However, apparently an „orphan“ radio flare is detected in 2007 that is not immediately visible in the optical light curve.



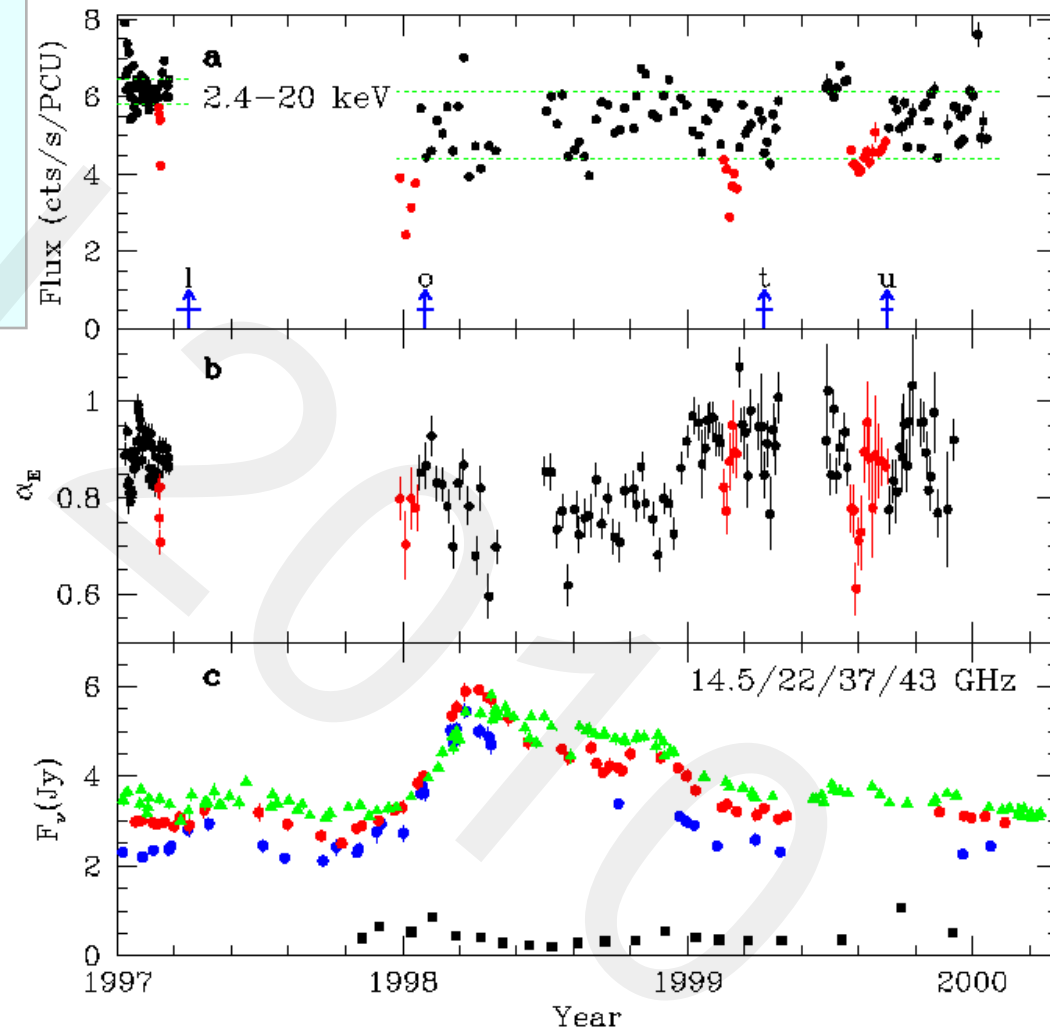


X-ray Continuum

☐ Ejections of new jet features are correlated with characteristic „dips“ in the X-ray light curve – likely due to disappearance of the inner part of the accretion disk.



3C390.3: Arshakian et al. 2010



3C120: Marscher et al. 2002, Chatterjee et al. 2009



Radio/Optical/X-ray in 3C120

- Joint modelling of radio, optical, and X-ray data in 3C120: radio flares and X-ray dips seem to originate near the accretion disk; optical flares are related to the region S1 located about 1 pc downstream.

Chatterjee et al. 2009:

X-ray, 43 GHz VLBI, and 37 GHz total flux density data

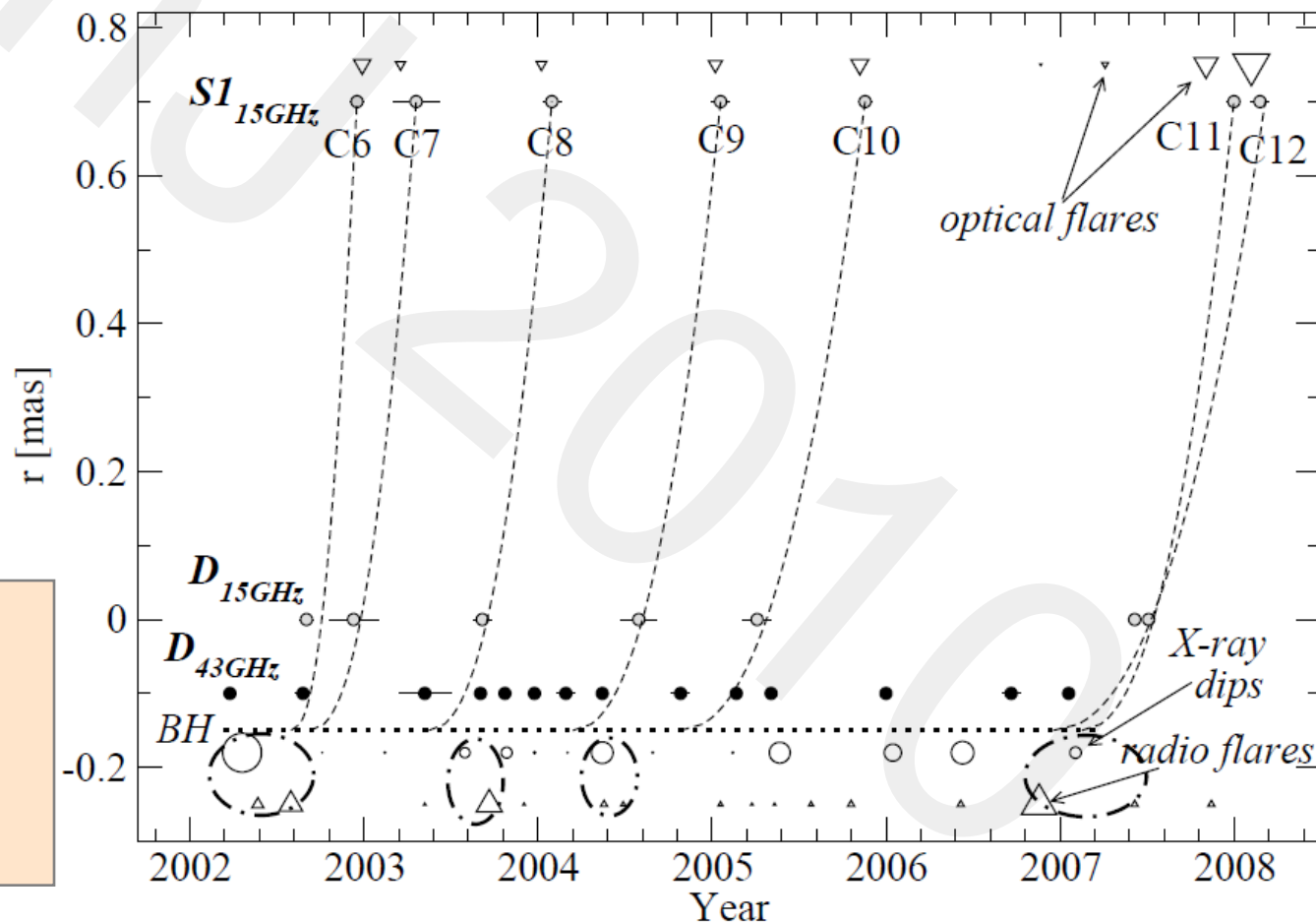
Tavares et al. 2010:

Optical and 15 GHz VLBI data

Jet acceleration modelling following the MHD acceleration model of Vlahakis & Königl 2003

Nuclear opacity and absolute geometry of the jet is determined from the core shift, according to Lobanov 1998.

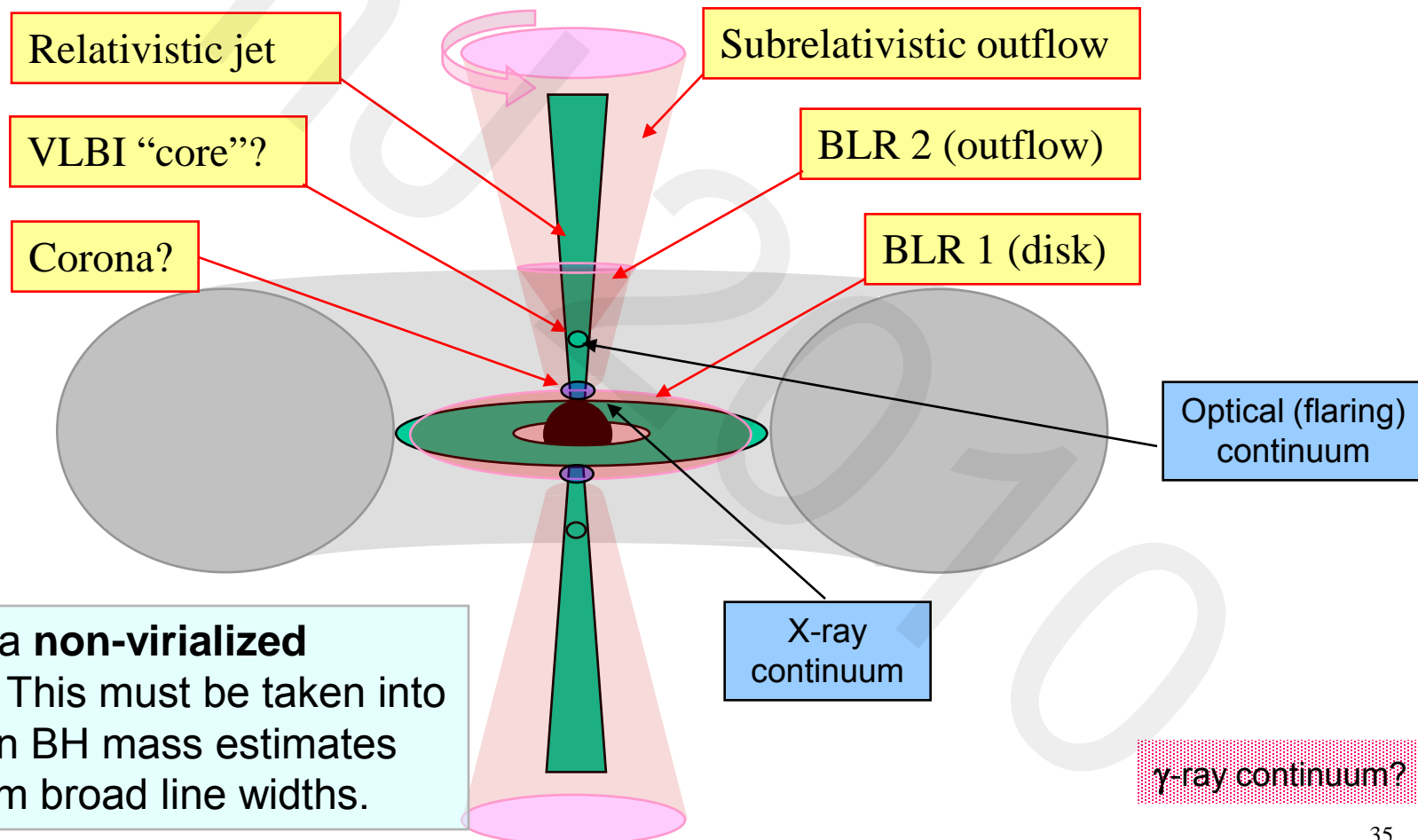
Instantaneous SEDs are likely to result from several physically different plasma components!





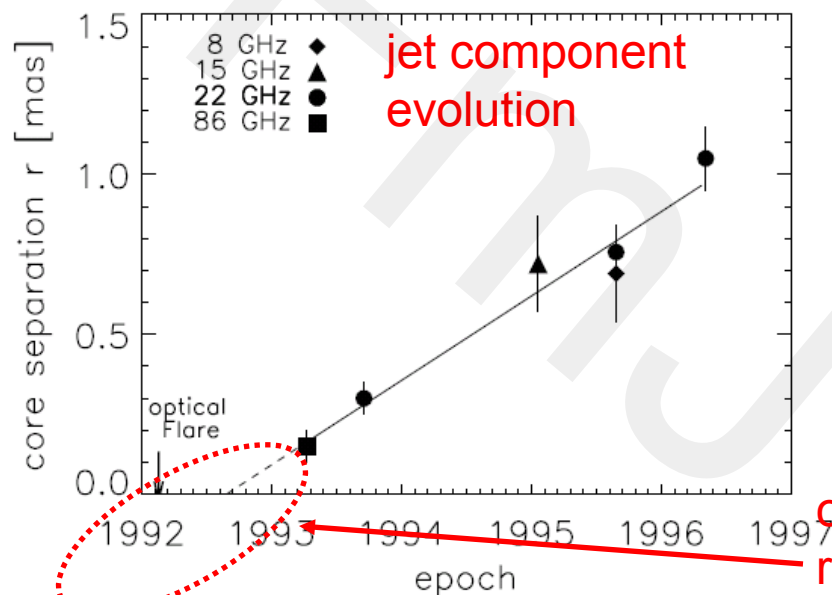
Radio-loud AGN

- ❑ In radio-loud AGN, relativistic jets may power a BLR associated with a subrelativistic outflow from the nucleus.

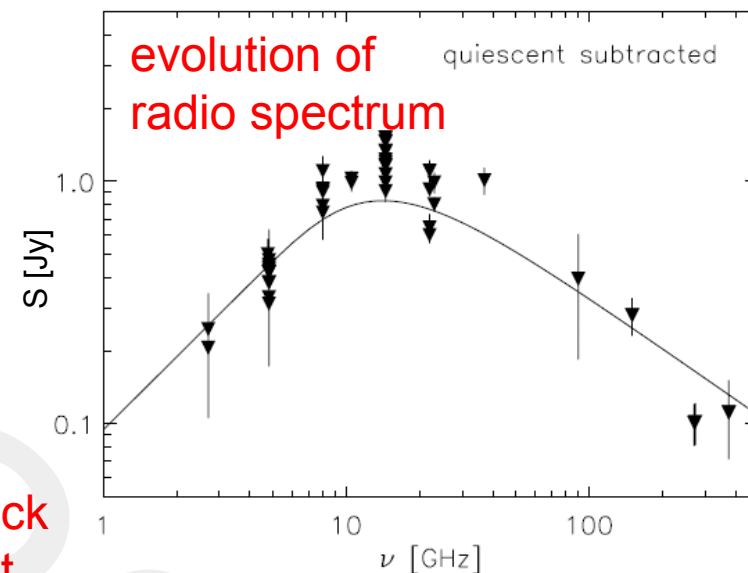




The γ -ray Connection

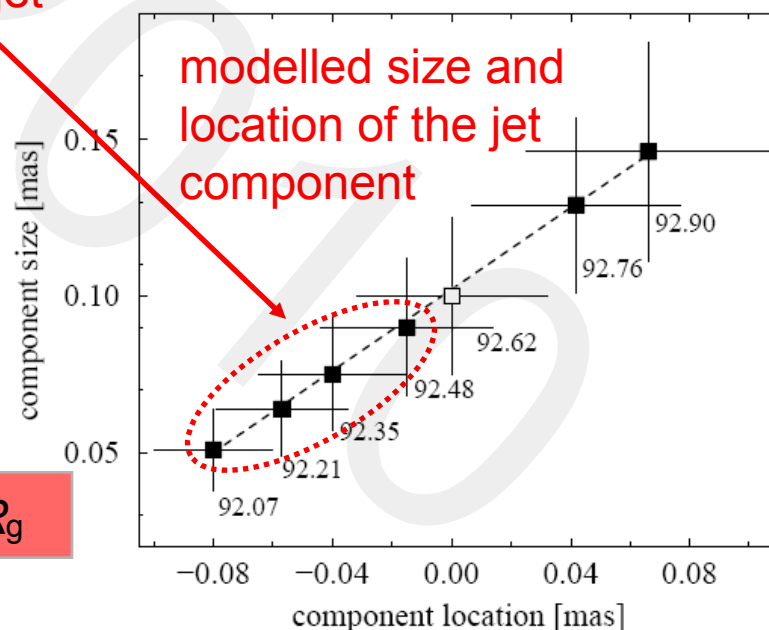


+



Lorentz factor, $\Gamma_j = 11.8$
Viewing angle, $\theta_j = 3.2$ deg
Doppler factor, $\delta_j = 16.4$
Opening angle, $\phi_j = 2.1$ deg
Magnetic field, $B_{\text{core}} = 0.2$ G

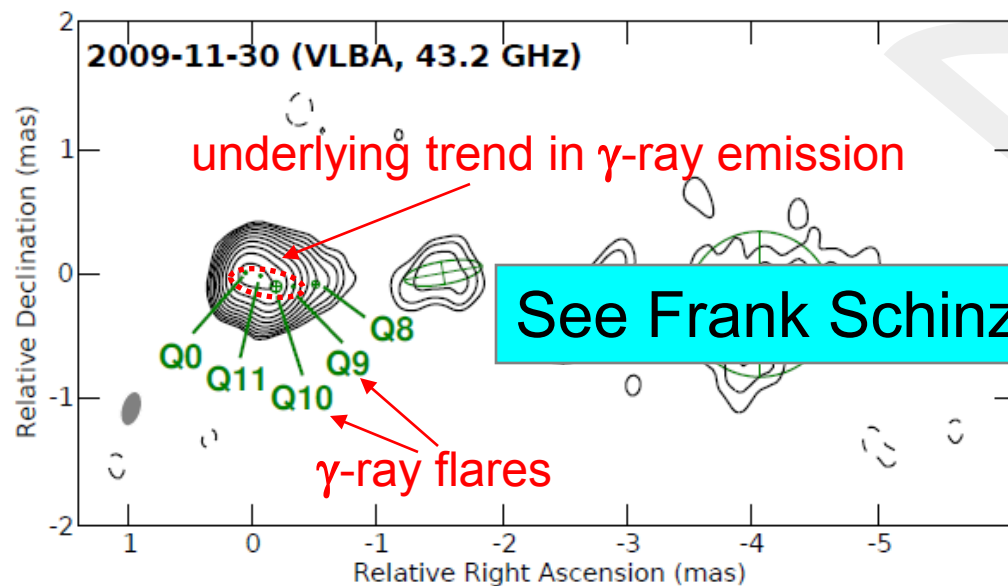
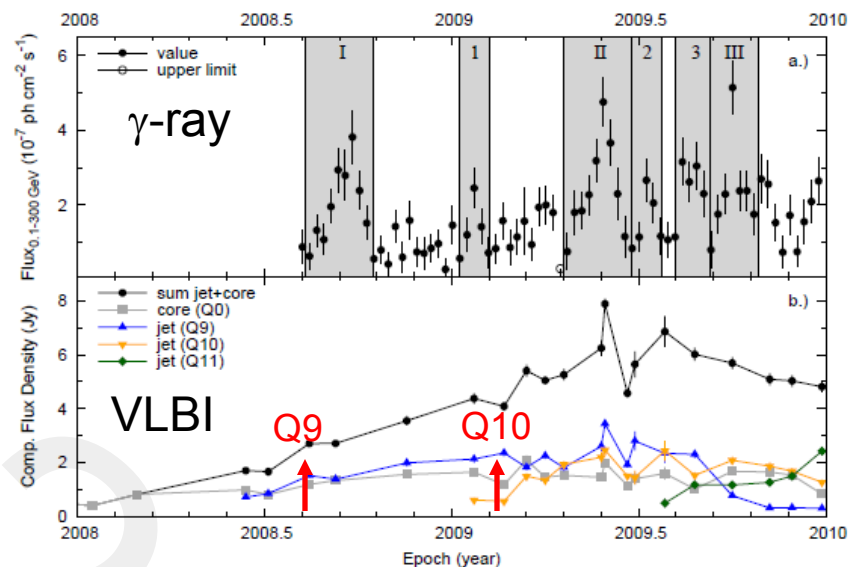
γ -ray flare occurred in the VLBI core, at $\sim 10^3 R_g$



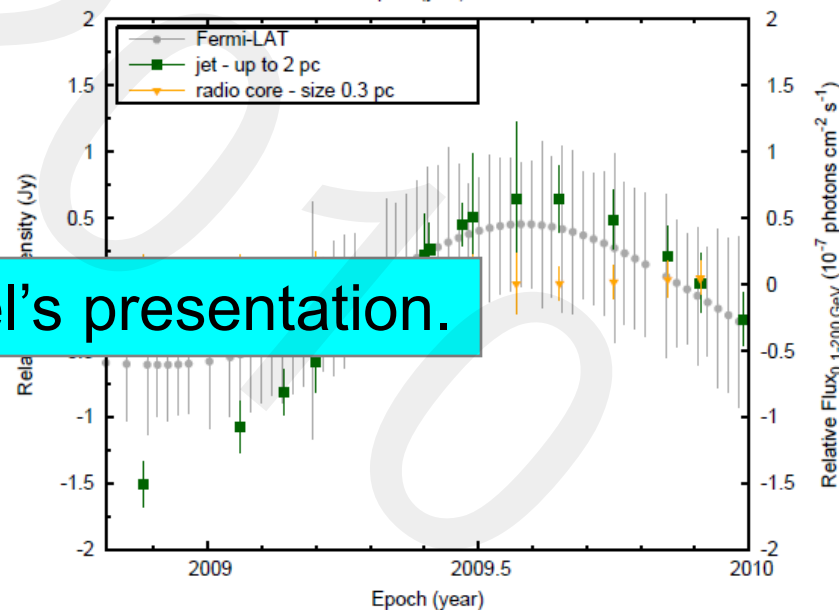


Jet γ -ray Continuum

□ The γ -ray emission in 3C345 is generated in a region of the jet of about 10 pc in extent, with individual flares likely associated with shocks moving through this region of the jet. The moving features also show a strong acceleration over this region.



See Frank Schinzel's presentation.





Summary

- ❑ Radio observations of jets in AGN jets probe physics and evolution of radio emission on scales of 10^2 – $10^9 R_g$.
- ❑ AGN jets can be divided into three qualitatively different regions:
 - collimation ($\sim 10^3 R_g$) and acceleration region (up to $10^6 R_g$; with likely release of strong, broad-band non-thermal continuum);
 - shock dominated region (up to $10^7 R_g$, with fast shocks pervading slower underlying flow);
 - instability dominated region (up to $10^9 R_g$, with Kelvin-Helmholtz instabilities shaping up the morphology and dynamics of the flow).
- ❑ Jets are major contributors to non-thermal continuum, and this contribution is not localised in a single region.
- ❑ VLBI offers an effective tool for accurate spatial localisation of sites of non-thermal continuum production, which is indispensable for modelling physical properties of blazars.